

## Regulation of 26S proteasome activity in pulmonary fibrosis

**Authors:** Nora Semren<sup>1</sup>, Vanessa Welk<sup>1#</sup>, Martina Korfei<sup>2#</sup>, Ilona E. Keller<sup>1</sup>, Isis E. Fernandez<sup>1</sup>, Heiko Adler<sup>3</sup>, Andreas Günther<sup>2,4</sup>, Oliver Eickelberg<sup>1</sup>, Silke Meiners<sup>1\*</sup>

### **Affiliations:**

<sup>1</sup>Comprehensive Pneumology Center (CPC), University Hospital, Ludwig-Maximilians University, Helmholtz Zentrum München, Munich, Member of the German Center for Lung Research (DZL), Germany.

<sup>2</sup>Department of Internal Medicine, Universities of Giessen and Marburg Lung Center (UGMLC), Justus-Liebig-University Giessen, Member of the German Center for Lung Research (DZL), Germany.

<sup>3</sup>Research Unit Gene Vectors, Helmholtz Zentrum München, Munich, Germany

<sup>4</sup>Agaplesion Lung Clinic Waldhof Elgershausen, Greifenstein, Germany, European IPF Network and European IPF Registry.

# both authors contributed equally

\*Corresponding author: Silke Meiners, Max-Lebsche Platz 31, 81377 Munich, Germany, Phone: 00498931874673, silke.meiners@helmholtz-muenchen.de

Contribution of each author: N.S. and S.M. conception and design of research; H.A., A.G., O.E. provided (clinical) samples and reagents; N.S., V.W., M.K., I.E.K., I.E.F. performed experiments; N.S., V.W., M.K., I.E.K., I.E.F. analyzed data; N.S., M.K. and S.M. interpreted

results; N.S. prepared figures; N.S. and S.M. drafted manuscript; N.S., V.W., M.K., O.E. and S.M. edited and revised manuscript; N.S., V.W., M.K., I.E.K., I.E.F., H.A., A.G., O.E. and S.M. approved final version.

Running head: Regulation of 26S proteasome activity in pulmonary fibrosis.

### 3.11 Pulmonary Fibrosis/Fibroblast Biology

Total word count: 3710 words

Word count abstract: 218words

#### At a Glance Commentary:

Scientific Knowledge on the Subject: The proteasome plays an important role in maintenance of protein homeostasis. While its dysregulation has been proposed to contribute to the pathogenesis of several chronic lung diseases, proteasome function in idiopathic pulmonary fibrosis has not been studied in detail so far.

What This Study Adds to the Field: We here provide evidence that the 26S proteasome is activated in human myofibroblasts *in vitro*, in experimental lung fibrosis *in vivo*, and in IPF lung tissue. Activation of the 26S proteasome is required for TGF- $\beta$  mediated myofibroblast differentiation suggesting that activation of 26S proteasome plays a pathogenic role in myofibroblast-driven fibrotic remodelling of the lung.

This article has an online data supplement, which is accessible from this issue's table of content online at [www.atsjournals.org](http://www.atsjournals.org)

**Abstract**

*Rationale:* The ubiquitin-proteasome system is critical for maintenance of protein homeostasis by degrading polyubiquitinated proteins in a spatially and timely controlled manner. Cell and protein homeostasis are altered upon pathological tissue remodelling. Dysregulation of the proteasome has been reported for several chronic diseases of the heart, brain, and lung. We hypothesized that proteasome function is altered upon fibrotic lung remodelling, thereby contributing to the pathogenesis of idiopathic pulmonary fibrosis (IPF).

*Methods:* To investigate proteasome function during myofibroblast differentiation, we treated lung fibroblasts with TGF- $\beta$  and examined proteasome composition and activity. For *in vivo* analysis, we used mouse models of lung fibrosis and fibrotic human lung tissue.

*Measurements and main results:* We demonstrate that induction of myofibroblast differentiation by TGF- $\beta$  involves activation of the 26S proteasome, which is critically dependent on the regulatory subunit Rpn6. Silencing of Rpn6 in primary human lung fibroblasts counteracted TGF- $\beta$ -induced myofibroblast differentiation. Activation of the 26S proteasome and increased expression of Rpn6 was detected during bleomycin-induced lung remodelling and fibrosis. Importantly, Rpn6 is overexpressed in myofibroblasts and basal cells of the bronchiolar epithelium in lungs of patients with IPF, which is accompanied by enhanced protein polyubiquitination.

*Conclusion:* Our study identifies Rpn6-dependent 26S proteasome activation as an essential feature of myofibroblast differentiation *in vitro* and *in vivo* and suggests an important role in IPF pathogenesis.

Word count: 218 words

Key words: IPF, proteasome, myofibroblast differentiation

## Introduction

Idiopathic pulmonary fibrosis (IPF) is an irreversible fibrotic disease of the lung in its worst form (1). It is characterized by progressive loss of alveolar structure, caused by excessive deposition of extracellular matrix (ECM) proteins, which adds to the loss of pulmonary elasticity and gas exchange, ultimately leading to organ failure and death (2). The pathomechanism of IPF involves repetitive severe injuries of alveolar epithelial cells together with dysregulated wound-healing responses contributing to fibrotic tissue remodelling of the lungs (3).

Transforming growth factor (TGF)- $\beta$  is the main profibrotic mediator inducing myofibroblast differentiation, an activation process resulting in ECM-secreting and  $\alpha$ -smooth muscle actin ( $\alpha$ SMA) expressing myofibroblasts. TGF- $\beta$  ligands and its receptors are highly induced in lungs of IPF patients and experimental models of pulmonary fibrosis (4, 5).

During differentiation and tissue remodelling, the ubiquitin-proteasome system degrades unwanted proteins thereby maintaining protein homeostasis and proper cellular function (6–11). For degradation, proteins are covalently tagged with polyubiquitin chains, which are mainly linked through their lysine 48 (K48) residues via a cascade of E1, E2, and E3 enzymes. Substrates are then recognized by the 26S proteasome and degraded into oligopeptides (12, 13). The 26S proteasome consists of a barrel-like proteolytic core particle, the 20S proteasome, and 19S regulatory complexes that are attached to one or both ends of the 20S (14). Three active sites within the 20S core particle cleave proteins after different amino acids. According to their cleavage site specificity they are named chymotrypsin-like (CT-L), trypsin-like (T-L), and caspase-like (C-L) active sites (15). The entry pore of the 20S barrel is usually closed to avoid uncontrolled degradation of proteins (15). This pore is opened by binding of the 19S forming singly-capped 26S or doubly-capped 30S proteasomes, respectively (14, 16, 17). The 19S

activator consists of more than 19 subunits, which enable binding of polyubiquitinated proteins, recycling of ubiquitin via deubiquitination, and ATP-dependent unfolding of protein chains to funnel them into the 20S catalytic core (18). The importance of the ubiquitin-proteasome system for maintenance of protein homeostasis in the lung is an emerging new concept for chronic lung diseases (7, 19, 20). While inhibition of the proteasome by specific proteasome inhibitors has been shown to provide antifibrotic effects in the bleomycin mouse model (21), regulation of proteasome function in lung fibrosis has not been studied in detail yet. Here, we hypothesized, that proteasome function is altered in fibrotic lung remodelling and contributes to the pathogenesis of IPF.

Some of the results of this study have been previously reported in the form of abstracts (22–26).

## **Materials and Methods**

### *Human Lung Tissue*

Explanted lungs or lobes from 13 patients with IPF (mean age  $\pm$  SD,  $50.3 \pm 7.9$  years; 7 females, 6 males) were obtained after lung transplantation and processed as detailed recently (27). Accordingly, atypical lung resections or lobes from 10 organ donors (mean age  $\pm$  SD,  $48.7 \pm 9.7$  years; 3 females, 5 males; in one case gender was unknown and in two cases gender and age were unknown) were obtained because of size incompatibilities and processed accordingly. All patients gave informed consent. All procedures were approved by local ethics committees (Justus-Liebig-University School of Medicine No. 31/93, 84/93, 29/01), the European IPF Registry (No. 111/08), and the University of Vienna School of Medicine (No. 076/2009).

### *Cell culture and gene silencing*

Primary human lung fibroblasts (phLF) were derived from peripheral normal lung tissue of explanted lungs from organ donors. Primary lines were established as previously reported (28, 29). The CCL206 mouse lung fibroblast cell line was obtained from ATCC and cultured under standard conditions. Details on the cell culture conditions and silencing experiments are provided in the Supplement.

### *Proteasome activity assays*

Proteasome activities were assayed as previously described (30) using specific luminogenic substrates (Proteasome-Glo Assay System, Promega) in hypoosmotic lysates supplemented with cOomplete protease (Roche) and phosphatase inhibitor (PhosStop, Roche). Native gel electrophoresis and ABP labelling of proteasome complexes was performed as detailed in the Supplement.

### *Immunohistochemistry (IHC)*

Immunohistochemical analysis of human and mouse lung tissue was performed as previously described and detailed in the Supplement (27).

### *Western blotting and antibodies*

Western blot analysis was performed as described previously (30) using 10% SDS-PAGE gels. Hypoosmotic lysates of CCL206 cells and mouse lungs, TSDG lysates of whole human tissue and phLF and RIPA lysates of phLF were prepared. The following antibodies were used for Western blot, native gel immunoblotting or immunohistochemistry: Rpn6 (Novus Biologicals), Rpt5 (Biomol), proteasome  $\beta$ 1 (Santa Cruz), proteasome  $\alpha$ 1-7 (Abcam), Ubiquitin K48 (Millipore),  $\beta$ -Actin (Sigma-Aldrich), Cyclin D1 (Cell Signaling), proteasome  $\beta$ 5 (Abcam),

Collagen-1 (Rockland), proteasome  $\alpha 3$  (Abcam), Cytokeratin-5 (Abcam),  $\alpha$ SMA (Abcam), and TTF1 (Abcam).

#### *RNA preparation and qRT PCR analysis*

Total RNA from cells was prepared using the Roti-Quick-Kit according to manufacturer's protocol (Carl Roth). 500 ng of RNA were reverse transcribed using random hexamers (Life Technologies) and M-MLV reverse transcriptase (Sigma-Aldrich). For quantitative PCR reactions, we used the SYBR Green LC480 System (Roche Diagnostics). mRNA expression was standardized to the hypoxanthine phosphoribosyl transferase gene or the 60S ribosomal protein L19 as a housekeeping gene (primer sequences available on request).

#### *Animal experiments*

Pathogen-free female C57BL/6 mice (10–12weeks old) were obtained from Charles River. All animal experiments were conducted according to international guidelines and were approved by the local administrative government. Initiation of pulmonary fibrosis and lung function analysis was performed as published and detailed in the Supplement (31, 32).

#### *Statistics*

Data are presented as means  $\pm$  SEMs and were considered statistically significant when  $p \leq 0.05$  (\* $p \leq 0.05$ , \*\* $p < 0.01$ , \*\*\* $p < 0.001$ ). Data were analysed using Prism 5 software (GraphPad Software) and statistical analysis was performed as detailed in the figure legends. Dixons outlier test was performed.

## Results

### *TGF- $\beta$ stimulates proteasome activity by Rpn6-dependent formation of 26S proteasomes*

To investigate a possible role of the proteasome in profibrotic TGF- $\beta$  signalling, we stimulated murine lung fibroblasts, i.e. CCL206 cells, with TGF- $\beta$  and analysed proteasome activities after 6, 24, and 48 hours of treatment. We observed a significant elevation in the chymotrypsin-like activity (CT-L) – the main proteolytic active site of the proteasome (33) - after 24h which further increased within 48h compared to untreated fibroblasts (Figure 1A). Subsequent addition of the proteasome inhibitor bortezomib counteracted TGF- $\beta$ -induced activation of the proteasome, thus confirming specificity of our activity assay (Supplementary Figure E1). Using native gel analysis, we resolved several active proteasome complexes using a fluorogenic CT-L substrate for in-gel activity assays (Figure 1B). Of note, TGF- $\beta$  stimulation increased formation of active 26S and 30S complexes as evidenced by immunoblotting of the native gels (Figure 1B and Supplementary Figure E2). Increased assembly of 26S and 30S proteasomes via the 19S subunit Rpn6 has recently been described for embryonic stem cell differentiation (34). We thus analysed whether Rpn6 mediates TGF- $\beta$ -induced assembly of 26S and 30S proteasome complexes. Western blot analysis revealed specific induction of Rpn6 expression after 48h of TGF- $\beta$  treatment in CCL206 cells while neither expression of the 19S ATPase subunit Rpt5 nor of the 20S subunits  $\alpha$ 1-7 were upregulated (Figure 1C). To validate the role of Rpn6 in TGF- $\beta$ -stimulated proteasome activity, we partially knocked down Rpn6 levels in murine lung fibroblasts and analysed proteasome activity after subsequent treatment of cells with TGF- $\beta$  for 48h. An approximate reduction of 50% of Rpn6 levels was well tolerated by the fibroblasts (Figure 1D and Supplementary Figure E3). Importantly, partial Rpn6 silencing neutralized TGF- $\beta$ -induced assembly and activation of 26S and 30S proteasome complexes as determined by

native gel activity assay and subsequent immunoblot detection of 20S ( $\alpha$ 1-7) and 19S complexes (Rpt5), respectively (Figure 1E). Reduced assembly and activity of 26S/30S proteasomes was reproducibly observed in four independent silencing experiments (Supplementary Figure E4). Silencing of Rpn6, however, did not affect the activity or amount of 20S proteasomes in CCL206 cells (Supplementary Figure E4 and E5). Our data thus indicate that Rpn6 is an essential 26S subunit which is required for TGF- $\beta$ -induced assembly of 26S and 30S proteasome complexes for ubiquitin-dependent protein degradation.

*Proteasome activity and Rpn6 expression is reversibly increased upon fibrotic remodelling of mouse lungs*

Having shown that TGF- $\beta$  stimulation of lung fibroblast involves 26S proteasome activation we next assayed proteasome activities in a mouse model of lung fibrosis. Mice were treated once with bleomycin by intratracheal instillation which resulted in acute inflammatory and tissue repair responses at day 7, followed by fibrotic remodelling of the lungs at day 14 and resolution of fibrosis until day 56 as determined by lung function analysis (Supplementary Figure E6). We observed a pronounced increase of all three proteasome activities at day 7 and in fibrotic lungs at day 14 after bleomycin challenge (Figure 2A). Increased proteasome activity, however, normalized to levels of control animals at day 56 when fibrosis was resolved (Figure 2A). Native gel analysis of fibrotic lungs revealed that the observed increase in proteasome activities at day 14 was due to enhanced formation of 26S/30S proteasome complexes as corroborated by immunoblotting for the catalytic 20S subunit  $\beta$ 1 and the 19S subunits Rpt5 and Rpn6 (Figure 2B). Moreover, Western blot analysis of these tissue lysates revealed significant upregulation specifically of Rpn6 in fibrotic mouse lungs while expression levels of 20S ( $\alpha$ 1-7) and other 19S

(e.g. Rpn5) subunits were not altered (Figure 2C). RNA levels of proteasomal subunits, however, were not significantly altered (Supplementary Figure E7).

To assess the dynamics and cellular source of Rpn6 expression in the course of reversible fibrotic remodelling, we analyzed the cellular composition of the lungs and expression of Rpn6 at days 7, 14, and 56 after bleomycin instillation in detail (Figure 3). Serial lung tissue sections were Masson-Goldner stained for overall collagen deposition and extent of fibrosis, and immunostained for Rpn6,  $\alpha$ SMA (myofibroblast and smooth muscle cell marker) and thyroid transcription factor 1 (TTF1), a marker for alveolar epithelial cells type II (AECII) and bronchiolar Clara cells. Of note, lung tissue of PBS treated control animals indicated no or only very weak staining for Rpn6. At day 7, Rpn6 expression was strongly upregulated in AECII and Clara cells that were also increased in number. Inflammatory cells were also detectable at this time point, but they expressed only moderate levels of Rpn6. During the fibrotic phase at day 14, hyperplastic AECIIs as well as myofibroblasts overexpressed Rpn6. At day 56, the alveolar structure was fully restored and expression levels of Rpn6 normalized. These data thus demonstrate that Rpn6 expression is upregulated in epithelial and fibroblast effector cells of reversible wound healing in the bleomycin model of lung fibrosis. Expression closely followed the course of proteasome activity suggesting that increased 26S/30S proteasome formation is responsible for the observed activation of the proteasome in fibrotic lungs at day 14.

We confirmed our findings in a mouse model of gamma-herpesvirus (MHV-68) induced irreversible pulmonary fibrosis (35): Formation of 26S/30S proteasomes was increased in lung tissue homogenates of virus-infected interferon- $\alpha$  receptor KO mice and expression of Rpn6 was elevated which correlated with the expression of the profibrotic marker  $\alpha$ SMA in these mice

(Supplementary Figures E8 and E9). These data suggest that activation of the 26S proteasome is an intrinsic feature of reversible and irreversible fibrotic remodelling of the lung.

#### *Rpn6 and ubiquitin levels are increased in IPF lungs*

Similar to our *in vitro* and *in vivo* data, we observed significant upregulation of Rpn6 in lung tissues of IPF patients compared to healthy donor lungs. Levels of Rpt5 were also elevated while expression of the 20S subunit  $\alpha 3$  was not altered (Figure 4A). Of note, RNA expression of proteasomal subunits was not significantly altered indicating regulation on the post-transcriptional level as observed for fibrotic mouse lungs (Supplementary Figure E10). We further observed an increase in K48-ubiquitinated proteins in IPF lung tissue compared to donor lungs (Figure 4A). High ubiquitin levels correlated positively with elevated Rpn6 expression (Figure 4B). Levels of K48-polyubiquitinated proteins increase either due to the accumulation of polyubiquitinated substrates (30) or as a result of enhanced turnover rates of proteins in metabolically active cells (36). We thus assayed proteasome activity in our IPF and donor lung tissues using the proteasome activity-based probe (ABP) MV151 combined with native gel analysis to resolve the different complexes (37). ABPs covalently bind to the active sites of the proteasome and can be detected by their attached fluorescent tag thus allowing quantification of active proteasome complexes. Proteasome activity was neither consistently inhibited nor activated in IPF lungs compared to donor tissue (Supplementary Figure E11). We noticed however, that in IPF samples, Rpn6 levels positively correlated with activation of 26S/30S proteasome activity (Figure 4C). This was not evident in donor samples and suggests some distinct activation of 26S proteasome activity in the diseased IPF lungs (Figure 4D). This notion is also supported by our immunohistological analysis of IPF lungs: In comparison to normal donor lungs, we observed pronounced upregulation of Rpn6 in myofibroblasts of fibroblast foci

as well as in abnormal overlying basal cells in diseased lungs (Figure 5), which are hallmarks of pulmonary remodelling in IPF (27). In addition, basal cells of IPF-bronchioles also showed enhanced immunostaining for Rpn6 (Figure 5). We also observed increased levels of K48-linked polyubiquitinated proteins in Rpn6-positive myofibroblasts and basal cells (Figure 6). To investigate whether proteasome activation is a general feature of fibrotic lung diseases or exclusive for IPF, we performed additional stainings of explanted lung tissues from patients with fibrotic non-specific interstitial pneumonia (fNSIP), sarcoidosis, and extrinsic allergic alveolitis (EAA). Of note, we did not observe any pronounced Rpn6 staining in NSIP and EAA lungs in any cell type and only weak expression of Rpn6 in epitheloid giant granulomas and some surrounding myofibroblasts in sarcoidosis (Supplementary Figure E12). Collectively, these data suggest that activation of ubiquitin-mediated protein degradation occurs specifically in areas of active fibrotic remodelling in IPF.

#### *Silencing of Rpn6 counteracts profibrotic differentiation of human lung fibroblasts*

To elucidate whether the observed upregulation of Rpn6 in myofibroblasts is related to TGF- $\beta$ -induced myogenic differentiation and proliferation, we silenced Rpn6 in primary human lung fibroblasts (pHLF) lines prepared from healthy organ donors in the absence or presence of TGF- $\beta$ . We first confirmed activation of 26S/30S proteasome activity by TGF- $\beta$  and its effective counteraction by partial silencing of Rpn6 (Figure 7A, Supplementary Figure E13). Rpn6 silencing slightly increased the amount of 20S proteasomes (Figure 7A, Supplementary Figure E13). Of note, partial Rpn6 silencing of about 40% counteracted TGF- $\beta$ -stimulated myofibroblast differentiation as revealed by qRT-PCR and Western blot analyses of the myogenic marker genes collagen I and fibronectin (Figures 7B, C and Supplementary Figure E14). Rpn6 silencing impaired basal expression of profibrotic markers in the absence of TGF- $\beta$

treatment (Figures 7B, C, and Supplementary Figure E14). These results were confirmed for collagen I in an additional set of Rpn6-silencing experiments using unstimulated pHLF (Figure 8). Partial knockdown of Rpn6 clearly increased K48-polyubiquitin and cyclin D1 protein levels demonstrating effective inhibition of ubiquitin-mediated protein degradation and indicating a G1 cell cycle arrest in these cells (38) (Figure 8). We observed similar changes for TGF- $\beta$  co-treated samples (Supplementary Figure E15). These findings are well in accordance with the growth inhibitory effects observed upon silencing of Rpn6 in murine lung fibroblast as detected by BrdU incorporation assays (Supplementary Figure E16). Our results thus identify an essential role for TGF- $\beta$  induced activation of 26S/30S proteasome complexes for myogenic growth and differentiation of lung fibroblasts.

## Discussion

Here, we show that the proteasome is activated in the process of TGF- $\beta$ -induced myofibroblast differentiation. Proteasome activation results from increased formation of 26S proteasomes, involving the 19S regulatory subunit Rpn6, and is required for myofibroblast differentiation. Increased proteasome activity and upregulation of Rpn6 was observed in both reversible and irreversible fibrotic remodelling of mouse lungs. In IPF lungs, Rpn6 expression was upregulated specifically in myofibroblasts and hyperplastic alveolar epithelial cells overlying fibroblast foci. Elevated levels of K48-polyubiquitin protein conjugates in these cells and the positive correlation of whole lung Rpn6 protein levels with K48-polyubiquitinated proteins suggest that activation of ubiquitin-dependent protein degradation by the 26S proteasome as a pathologic feature of fibrotic remodelling occurs specifically in IPF. The ubiquitin-proteasome system and TGF- $\beta$  signalling are closely linked by the ubiquitin-mediated degradation of signal mediators of the TGF- $\beta$  pathway (39). Here, we show for the first time that TGF- $\beta$  activates the ubiquitin-

proteasome system during the process of myofibroblast differentiation. We observed increased formation of highly active 26S proteasome complexes in pulmonary fibroblasts which was dependent on the 19S subunit Rpn6. Cryo-EM structures of the 26S proteasome have identified Rpn6 as a molecular clamp stabilizing the interaction between the 19S regulatory particle and the 20S catalytic core (40). The particular relevance of Rpn6 for 26S formation is supported by the recent finding that increased assembly of 26S complexes depended on Rpn6 as shown by overexpression, knockdown, and genetic deletion analysis in human embryonic stem cells and *C. elegans*, respectively (34, 41). In our study, partial knockdown of Rpn6 prevented TGF- $\beta$  mediated formation of 26S proteasomes and counteracted growth and differentiation of primary human lung fibroblasts into myofibroblasts. In addition, increased protein levels of Rpn6 correlated with 26S proteasome activation in pulmonary fibroblasts and fibrotic mouse lungs. Strongly elevated expression of Rpn6 was also observed in tissue homogenates of IPF lungs, as well as in myofibroblasts of fibrotic foci, of human IPF lungs, whereas immunostaining for Rpn6 was absent in lung tissues from patients with fibrotic NSIP or EAA, or only faintly expressed in some myofibroblasts in close proximity to granulomas in the lungs of sarcoidosis patients. A recent study also showed increased levels of proteasomes in IPF and sarcoidosis lungs (42). While overall proteasome activity was not altered in IPF lungs, increased levels of polyubiquitinated proteins correlated positively with Rpn6 upregulation both in tissue homogenates and in myofibroblasts of IPF tissue. These data thus indicate that activation of ubiquitin-dependent degradation by the 26S proteasome is an integral part of myofibroblast differentiation and fibrotic tissue remodelling. As we also observed increased levels of Rpn6 in activated AECII and bronchial Clara cells of bleomycin-challenged mice and in hyperplastic basal cells in close proximity to fibroblast foci of IPF lungs, it is tempting to speculate that these

activated epithelial cells contribute to the abnormal, exaggerated production of profibrotic signals in IPF and thus require enhanced formation and activation of 26S proteasomes. Moreover, 26S proteasome activation may be a general feature of cellular activation and tissue remodelling in the lung. The observation that epidermal growth factor (EGF) signalling activates the proteasome and enhances ubiquitin-mediated protein degradation in *C. elegans* supports this notion (43). Similarly, hypertrophic growth of cardiomyocytes involves activation of ubiquitin-mediated protein turnover via the 26S proteasome (44). Furthermore, a recent study unravelled a previously unknown link between mTOR mediated growth signalling and 26S proteasome activation (9). Taken together these data support the concept that signal-induced formation of 26S proteasomes represents a novel regulatory mechanism that allows the cell to rapidly adjust ubiquitin-mediated protein degradation in order to maintain protein homeostasis during differentiation and remodeling (14, 19, 45).

Our results also indicate that targeting the formation of 26S proteasome complexes represents a novel therapeutic approach to interfere with pulmonary myofibroblast differentiation. This would be more specific than the use of catalytic proteasome inhibitors that inactivate the proteolytic active sites of the 20S. Proteasome inhibitors have previously been shown to interfere with myofibroblast growth, differentiation and also fibrotic organ remodelling in different organs such as heart, skin, kidney and lung (21, 46–49). For the lung, however, there are conflicting data regarding the antifibrotic effects of proteasome inhibitors in the bleomycin model of lung fibrosis: While Fineschi et al. reported that treatment with the clinically approved proteasome inhibitor bortezomib did not show any protective effects in bleomycin-treated mice (48), Mutlu et al. observed that bortezomib promoted tissue repair and prevented lung fibrosis in response to bleomycin challenge. They also reported, however, that application of both drugs, bortezomib

and bleomycin, at the same time, resulted in excess mortality of these mice (21). These data suggest that there is only a small therapeutic window for catalytic proteasome inhibitors. This has also been reported for other disease applications and clearly hampers the use of these drugs beyond tumour therapy (50, 51). In addition, testing of proteasome inhibitors in the bleomycin model of pulmonary fibrosis has its limitations and its comparison to IPF pathology has been highly controversial (52, 53). As also shown in our study here, bleomycin instillation induces acute lung injury with a reparative wound healing response but it lacks the irreversible formation of fibroblast foci and bronchiolized alveolar airspaces which both are hallmarks of IPF (1, 53). In clear contrast to IPF, fibrotic tissue remodelling and lung function decline are reversible and fully restored over time.

Therapeutic application of catalytic proteasome inhibitors for treatment of pulmonary fibrosis is a narrow bridge between beneficial antifibrotic and harmful cytotoxic effects as indiscriminate inhibition of the proteolytic sites of all 20S containing proteasomal complexes kills the cell (50, 55). Current drug development thus aims to develop site-specific inhibitors of the proteasome or to target ubiquitin-mediated protein degradation further upstream by interfering with specific E3 ligases or deubiquitinases (56, 57). A completely novel targeting approach that seeks to inhibit the interaction of proteasomal regulators with the 20S catalytic core is based on the recent realization that different proteasomal complexes have diverse cellular functions (19, 45, 58–60). As there are no established drugs available yet, knockdown of single proteasome regulators or of components thereof, such as Rpn6, allows validation of this targeting approach. Specific interference with 26S proteasome function, as shown here for Rpn6 silencing, might offer a new therapeutic treatment strategy to counteract activation of specific 26S proteasome complexes in areas of active fibrotic remodelling in IPF.

To conclude, we here provide evidence that the 26S proteasome is activated in myofibroblasts *in vitro*, in experimental lung fibrosis *in vivo*, and in IPF lung tissue. We propose that 26S proteasome activation and induction of Rpn6 is a novel pathomechanism during fibrotic organ remodelling. Activation of the 26S proteasome is well in line with the emerging concept of fine-tuned regulation of proteasomal protein degradation for cell and tissue homeostasis (8, 10, 14). Impairment of 26S proteasome activation by silencing of the regulatory subunit Rpn6 inhibited myofibroblast differentiation of primary human lung fibroblasts and may thus represent a novel approach to counteract activation of 26S proteasome complexes in areas of active fibrotic remodelling, thereby potentially interfering with the pathogenesis of IPF.

## **Acknowledgements**

We thank Christina Lukas for excellent technical assistance. Nora Semren was funded by the Helmholtz Graduate School “Lung Biology and Disease”.

## References

1. Raghu G, Collard HR, Egan JJ, Martinez FJ, Behr J, Brown KK, Colby T V, Cordier J-F, Flaherty KR, Lasky J a, Lynch D a, Ryu JH, Swigris JJ, Wells AU, Ancochea J, Bouros D, Carvalho C, Costabel U, Ebina M, Hansell DM, Johkoh T, Kim DS, King TE, Kondoh Y, Myers J, Müller NL, Nicholson AG, Richeldi L, Selman M, *et al.* An official ATS/ERS/JRS/ALAT statement: idiopathic pulmonary fibrosis: evidence-based guidelines for diagnosis and management. *Am J Respir Crit Care Med* 2011;183:788–824.
2. Fernandez IE, Eickelberg O. New cellular and molecular mechanisms of lung injury and fibrosis in idiopathic pulmonary fibrosis. *Lancet* 2012;380:680–8.
3. Wynn TA. Integrating mechanisms of pulmonary fibrosis. *J Exp Med* 2011;208:1339–50.
4. Wynn TA, Ramalingam TR. Mechanisms of fibrosis: therapeutic translation for fibrotic disease. *Nat Med* 2012;18:1028–40.
5. Duffield JS, Lucher M, Thannickal VJ, Wynn T a. Host responses in tissue repair and fibrosis. *Annu Rev Pathol* 2013;8:241–76.
6. Powers ET, Balch WE. Diversity in the origins of proteostasis networks - a driver for protein function in evolution. *Nat Rev Mol Cell Biol* 2013;14:237–48.
7. Balch WE, Morimoto RI, Dillin A, Kelly JW. Adapting proteostasis for disease intervention. *Science* 2008;319:916–9.

8. Vilchez D, Simic MS, Dillin A. Proteostasis and aging of stem cells. *Trends Cell Biol* 2014;24:161–70.
9. Zhang Y, Nicholatos J, Dreier JR, Ricoult SJH, Widenmaier SB, Hotamisligil GS, Kwiatkowski DJ, Manning BD. Coordinated regulation of protein synthesis and degradation by mTORC1. *Nature* 2014;513:440–3.
10. Buszczak M, Signer RAJ, Morrison SJ. Cellular Differences in Protein Synthesis Regulate Tissue Homeostasis. *Cell* 2014;159:242–251.
11. Finley D. Recognition and processing of ubiquitin-protein conjugates by the proteasome. *Annu Rev Biochem* 2009;78:477–513.
12. Ciechanover A. Intracellular protein degradation: from a vague idea thru the lysosome and the ubiquitin-proteasome system and onto human diseases and drug targeting. *Cell Death Differ* 2005;12:1178–90.
13. Teixeira LK, Reed SI. Ubiquitin ligases and cell cycle control. *Annu Rev Biochem* 2013;82:387–414.
14. Bhattacharyya S, Yu H, Mim C, Matouschek A. Regulated protein turnover: snapshots of the proteasome in action. *Nat Rev Mol Cell Biol* 2014;15:122–33.
15. Groll M, Bajorek M, Köhler a, Moroder L, Rubin DM, Huber R, Glickman MH, Finley D. A gated channel into the proteasome core particle. *Nat Struct Biol* 2000;7:1062–7.

16. Tomko RJ, Hochstrasser M. Molecular architecture and assembly of the eukaryotic proteasome. *Annu Rev Biochem* 2013;82:415–45.
17. Lander GC, Estrin E, Matyskiela ME, Bashore C, Nogales E, Martin A. Complete subunit architecture of the proteasome regulatory particle. *Nature* 2012;
18. Liu C-W, Jacobson AD. Functions of the 19S complex in proteasomal degradation. *Trends Biochem Sci* 2013;38:103–10.
19. Meiners S, Keller IE, Semren N, Caniard A. Regulation of the Proteasome: Evaluating the Lung Proteasome as a New Therapeutic Target. *Antioxid Redox Signal* 2014;00:1–20.
20. Balch WE, Sznajder JI, Budinger S, Finley D, Laposky AD, Cuervo AM, Benjamin IJ, Barreiro E, Morimoto RI, Postow L, Weissman AM, Gail D, Banks-Schlegel S, Croxton T, Gan W. Malfolded protein structure and proteostasis in lung diseases. *Am J Respir Crit Care Med* 2014;189:96–103.
21. Mutlu GM, Budinger GRS, Wu M, Lam AP, Zirk A, Rivera S, Urich D, Chiarella SE, Go LHT, Ghosh AK, Selman M, Pardo A, Varga J, Kamp DW, Chandel NS, Sznajder JI, Jain M. Proteasomal inhibition after injury prevents fibrosis by modulating TGF- $\beta$ (1) signalling. *Thorax* 2012;67:139–46.
22. Semren N, Fernandez IE, Günther A, Eickelberg O. Proteasome function in lung fibrosis. *Abstr MLC* 2013;
23. Semren N, Fernandez IE, Günther A, Eickelberg O, Meiners S. Regulation of the proteasome in lung fibrosis. *Abstr ERS* 2013;

24. Semren N, Welk V, Korfei M, Fernandez IE, Günther A, Eickelberg O, Meiners S. Proteasome function in lung fibrosis. *Abstr ERS* 2014;
25. Semren N, Welk V, Korfei M, Fernandez IE, Günther A, Eickelberg O, Meiners S. Altered proteasome function in lung fibrosis. *Abstr ATS* 2014;
26. Semren N, Welk V, Korfei M, Fernandez IE, Günther A, Eickelberg O, Meiners S. Altered proteasome function in lung fibrosis. *Abstr DZL Meet* 2014;
27. Korfei M, Schmitt S, Ruppert C, Henneke I, Markart P, Loeh B, Mahavadi P, Wygrecka M, Klepetko W, Fink L, Bonniaud P, Preissner KT, Lochnit G, Schaefer L, Seeger W, Guenther A. Comparative proteomic analysis of lung tissue from patients with idiopathic pulmonary fibrosis (IPF) and lung transplant donor lungs. *J Proteome Res* 2011;10:2185–205.
28. Jordana M, Newhouse MT, Gauldie J. Alveolar macrophage/peripheral blood monocyte-derived factors modulate proliferation of primary lines of human lung fibroblasts. *J Leukoc Biol* 1987;42:51–60.
29. Jordana M, Befus AD, Newhouse MT, Bienenstock J, Gauldie J. Effect of histamine on proliferation of normal human adult lung fibroblasts. *Thorax* 1988;43:552–8.
30. Van Rijt SH, Keller IE, John G, Kohse K, Yildirim AÖ, Eickelberg O, Meiners S. Acute cigarette smoke exposure impairs proteasome function in the lung. *Am J Physiol Lung Cell Mol Physiol* 2012;303:L814–23.

31. John G, Kohse K, Orasche J, Reda A, Schnelle-Kreis J, Zimmermann R, Schmid O, Eickelberg O, Yildirim AÖ. The composition of cigarette smoke determines inflammatory cell recruitment to the lung in COPD mouse models. *Clin Sci (Lond)* 2014;126:207–21.
32. Aumiller V, Balsara N, Wilhelm J, Günther A, Königshoff M. WNT/ $\beta$ -catenin signaling induces IL-1 $\beta$  expression by alveolar epithelial cells in pulmonary fibrosis. *Am J Respir Cell Mol Biol* 2013;49:96–104.
33. Marques AJ, Palanimurugan R, Matias AC, Ramos PC, Dohmen RJ. Catalytic mechanism and assembly of the proteasome. *Chem Rev* 2009;109:1509–36.
34. Vilchez D, Boyer L, Morantte I, Lutz M, Merkwirth C, Joyce D, Spencer B, Page L, Masliah E, Berggren WT, Gage FH, Dillin A. Increased proteasome activity in human embryonic stem cells is regulated by PSMD11. *Nature* 2012;489:304–8.
35. Mora AL, Woods CR, Garcia A, Xu J, Rojas M, Speck SH, Roman J, Brigham KL, Stecenko AA. Lung infection with gamma-herpesvirus induces progressive pulmonary fibrosis in Th2-biased mice. *Am J Physiol Lung Cell Mol Physiol* 2005;289:L711–21.
36. Zhang H, Xing L. Ubiquitin e3 ligase itch negatively regulates osteoblast differentiation from mesenchymal progenitor cells. *Stem Cells* 2013;31:1574–83.
37. Cravatt BF, Wright AT, Kozarich JW. Activity-based protein profiling: from enzyme chemistry to proteomic chemistry. *Annu Rev Biochem* 2008;77:383–414.
38. Yang K, Hitomi M, Stacey DW. Variations in cyclin D1 levels through the cell cycle determine the proliferative fate of a cell. *Cell Div* 2006;1:32.

39. Soond SM, Chantry A. How ubiquitination regulates the TGF- $\beta$  signalling pathway: new insights and new players: new isoforms of ubiquitin-activating enzymes in the E1-E3 families join the game. *Bioessays* 2011;33:749–58.
40. Pathare GR, Nagy I, Bohn S, Unverdorben P, Hubert A, Körner R, Nickell S, Lasker K, Sali A, Tamura T, Nishioka T, Förster F, Baumeister W, Bracher A. The proteasomal subunit Rpn6 is a molecular clamp holding the core and regulatory subcomplexes together. *Proc Natl Acad Sci U S A* 2012;109:149–54.
41. Vilchez D, Morante I, Liu Z, Douglas PM, Merkwirth C, Rodrigues APC, Manning G, Dillin A. RPN-6 determines *C. elegans* longevity under proteotoxic stress conditions. *Nature* 2012;489:263–8.
42. Baker TA, Bach HH, Gamelli RL, Love RB, Majetschak M, Bach Iv HH, Gamelli RL, Love RB, Majetschak M, Bach HH, Gamelli RL, Love RB, Majetschak M. Proteasomes in lungs from organ donors and patients with end-stage pulmonary diseases. *Physiol Res* 2014;63:311–9.
43. Liu G, Rogers J, Murphy CT, Rongo C. EGF signalling activates the ubiquitin proteasome system to modulate *C. elegans* lifespan. *EMBO J* 2011;30:2990–3003.
44. Mearini G, Schlossarek S, Willis MS, Carrier L. The ubiquitin-proteasome system in cardiac dysfunction. *Biochim Biophys Acta - Mol Basis Dis* 2008;
45. Schmidt M, Finley D. Regulation of proteasome activity in health and disease. *Biochim Biophys Acta* 2014;1843:13–25.

46. Meiners S, Hocher B, Weller A, Laule M, Stangl V, Guenther C, Godes M, Mrozikiewicz A, Baumann G, Stangl K. Downregulation of matrix metalloproteinases and collagens and suppression of cardiac fibrosis by inhibition of the proteasome. *Hypertension* 2004;44:471–7.
47. Koca SS, Ozgen M, Dagli F, Tuzcu M, Ozercan IH, Sahin K, Isik A. Proteasome inhibition prevents development of experimental dermal fibrosis. *Inflammation* 2012;35:810–7.
48. Fineschi S, Bongiovanni M, Donati Y, Djaafar S, Naso F, Goffin L, Argiroffo CB, Pache J-C, Dayer J-M, Ferrari-Lacraz S, Chizzolini C. In vivo investigations on anti-fibrotic potential of proteasome inhibition in lung and skin fibrosis. *Am J Respir Cell Mol Biol* 2008;39:458–65.
49. Fineschi S, Reith W, Guerne PA, Dayer J-M, Chizzolini C. Proteasome blockade exerts an antifibrotic activity by coordinately down-regulating type I collagen and tissue inhibitor of metalloproteinase-1 and up-regulating metalloproteinase-1 production in human dermal fibroblasts. *FASEB J* 2006;20:562–4.
50. Meiners S, Ludwig A, Stangl V, Stangl K. Proteasome inhibitors: poisons and remedies. *Med Res Rev* 2008;28:309–27.
51. Di Napoli M, McLaughlin B. The ubiquitin-proteasome system as a drug target in cerebrovascular disease: therapeutic potential of proteasome inhibitors. *Curr Opin Investig Drugs* 2005;6:686–99.

52. Moore BB, Lawson WE, Oury TD, Sisson TH, Raghavendran K, Hogaboam CM. Animal models of fibrotic lung disease. *Am J Respir Cell Mol Biol* 2013;
53. Moeller A, Ask K, Warburton D, Gauldie J, Kolb M. The bleomycin animal model: a useful tool to investigate treatment options for idiopathic pulmonary fibrosis? *Int J Biochem Cell Biol* 2008;40:362–82.
54. Moore BB, Hogaboam CM. Murine models of pulmonary fibrosis. *Am J Physiol Lung Cell Mol Physiol* 2008;294:L152–L160.
55. Weiss CH, Budinger GRS, Mutlu GM, Jain M. Proteasomal regulation of pulmonary fibrosis. *Proc Am Thorac Soc* 2010;7:77–83.
56. Eldridge AG, O'Brien T. Therapeutic strategies within the ubiquitin proteasome system. *Cell Death Differ* 2010;17:4–13.
57. D'Arcy P, Brnjic S, Olofsson MH, Fryknäs M, Lindsten K, De Cesare M, Perego P, Sadeghi B, Hassan M, Larsson R, Linder S. Inhibition of proteasome deubiquitinating activity as a new cancer therapy. *Nat Med* 2011;17:1636–40.
58. Lander GC, Martin A, Nogales E. The proteasome under the microscope: The regulatory particle in focus. *Curr Opin Struct Biol* 2013;
59. Tanaka K, Mizushima T, Saeki Y. The proteasome: molecular machinery and pathophysiological roles. *Biol Chem* 2012;393:217–234.

60. Gaczynska M, Osmulski PA. Targeting Protein-Protein Interactions in the Proteasome Super-Assemblies. *Curr Top Med Chem* 2015;doi:10.2174/1568026615666150519103206.

## Figure legends

**Fig. 1.** TGF- $\beta$  stimulates proteasome activity and 26S formation in CCL206 lung fibroblasts via Rpn6. **(A)** Chymotrypsin-like (CT-L) proteasome activity in hypoosmotic cell lysates of fibroblasts treated with TGF- $\beta$  for 6h, 24h, and 48h (Mean  $\pm$  SEM.  $n = 4$  for 6h and 24h,  $n = 7$  for 48h. One-way ANOVA, Dunnett's Multiple Comparison Test). **(B)** Native gel analysis of hypoosmotic cell lysates after treatment with TGF- $\beta$  for 48h with subsequent CT-L activity overlay assay and immunoblotting for the 20S alpha subunits  $\alpha 1-7$  and the 19S regulatory subunit Rpt5. Densitometry analysis of 26S/30S levels obtained from  $\alpha 1-7$  immunoblots (Mean  $\pm$  SEM.  $n = 3$ , Paired t-test). **(C)** Western blot analysis of hypoosmotic CCL206 lysates after treatment with TGF- $\beta$  for 48h for the 20S alpha subunits  $\alpha 1-7$  and the 19S regulatory subunits Rpn6 and Rpt5 using  $\beta$ -actin to confirm equal loading. Densitometric analysis was performed for  $\beta$ -actin normalized signals of  $\alpha 1-7$ , Rpn6 and Rpt5, and compared to untreated controls (Mean  $\pm$  SEM.  $n = 3$ . One-way ANOVA, Dunnett's Multiple Comparison Test) **(D)** Western blot analysis of hypoosmotic lysates of CCL206 fibroblasts after transfection of scrambled or Rpn6-specific siRNAs followed by treatment with TGF- $\beta$  for 48h. Densitometric analysis was performed for  $\beta$ -actin normalized Rpn6 signals (Mean  $\pm$  SEM.  $n = 4$ . One-way ANOVA Bonferroni-Multiple Comparison Test). **(E)** Representative native gel analysis of cell lysates of CCL206 fibroblasts after Rpn6 knockdown and treatment with TGF- $\beta$  for 48h with subsequent in gel CT-L activity assay and immunoblotting for the 20S subunits  $\alpha 1-7$  and the 19S subunit Rpt5. Densitometric analysis of 26S/30S levels as represented by Rpt5 immunoblot signals was performed for four independent silencing experiments (Mean  $\pm$  SEM.  $n = 4$ . Two-tailed Mann Whitney Test).

**Fig. 2.** Proteasome activity is reversibly increased upon fibrotic lung remodeling in the bleomycin mouse model of pulmonary fibrosis. **(A)** Proteasome activity was assayed in hypoosmotic lysates of whole lung tissue of C57BL/6N mice 7, 14, and 56 days after treatment with bleomycin and compared to the PBS-treated control group (Mean  $\pm$  SEM.  $n = 5-15$  per group. Two-tailed Mann Whitney Test, Dixons outlier test was performed and the outlier is shown in brackets). **(B)** Native gel analysis of hypoosmotic lysates of whole lung tissue at day 14 after bleomycin instillation with subsequent in-gel CT-L activity assay and immunoblotting for the 20S  $\beta$ 1 subunit and the 19S regulatory subunits Rpt5 and Rpn6. Loading of purified 20S proteasomes confirmed 20S proteasome activity in lung tissue lysates **(C)** Western blot of hypoosmotic lysates of whole lung tissue of C57BL/6N mice 14 days after bleomycin instillation for Rpn6,  $\beta$ 1-7, Rpt5 and  $\beta$ -actin, and densitometric analysis of normalized expression data (Mean  $\pm$  SEM.  $n = 6$  per group. One-way ANOVA Dunnett's Multiple Comparison Test).

**Fig. 3.** Rpn6 expression is upregulated in hyperplastic AECII, Clara cells, and myofibroblasts during reversible fibrotic remodeling in bleomycin induced pulmonary fibrosis. Paraffin-embedded lung tissue sections of PBS treated control animals or animals, which were sacrificed 7, 14 or 56 days after bleomycin instillation, were analyzed by Masson-Goldner staining for fibrotic remodelling (red staining for keratin and muscle fibres, blue/green collagen, pink cytoplasm, brown/black: nucleus). Expression of  $\alpha$ SMA (marker for myofibroblasts and smooth muscle cells) and Rpn6 is indicated in red and expression of TTF1 (marker for AECII and Clara cells) in brown color. Of note, lung tissue of PBS treated control animals indicate no or only faint staining for Rpn6. Weak

immunoreactivity for Rpn6 was also observed in mice lungs 56 days after bleomycin instillation. Pictures show representative stainings from 3-6 animals per group.

**Fig. 4.** Expression of Rpn6 and K48-polyubiquitinated proteins is increased in human IPF lungs.

(A) Western blot analysis of RIPA lysates of whole lung tissue of donor and IPF lungs. Expression of Rpn6, Rpt5, K48-polyubiquitinated proteins,  $\alpha$ SMA and the  $\alpha$ 3 subunit of the 20S proteasome was quantified by densitometry after normalization to  $\beta$ -actin (Mean  $\pm$  SEM.  $n = 11-13$  per group. Two-tailed Mann Whitney Test). (B) Correlation analysis of normalized expression of K48-polyubiquitinated proteins and Rpn6 from the Western blot data. Donor and IPF values were pooled (Two-tailed Spearman correlation,  $r = 0.508$ ,  $p = 0.013$ ). Separate correlation analyses of IPF (C) and donor lungs (D) for the amount of active 26S/30S proteasomes as obtained from densitometric analysis of ABP native gel analysis (Supplementary Figure E11), and  $\beta$ -actin normalized Rpn6 expression levels obtained from the western blot (Two-tailed Spearman correlation, IPF  $r = 0.648$ ,  $p = 0.017$ ; Donor  $r = -0.127$ ,  $p = 0.711$ ).

**Fig. 5.** Rpn6 is overexpressed in myofibroblasts and hyperplastic basal cells in human IPF lungs.

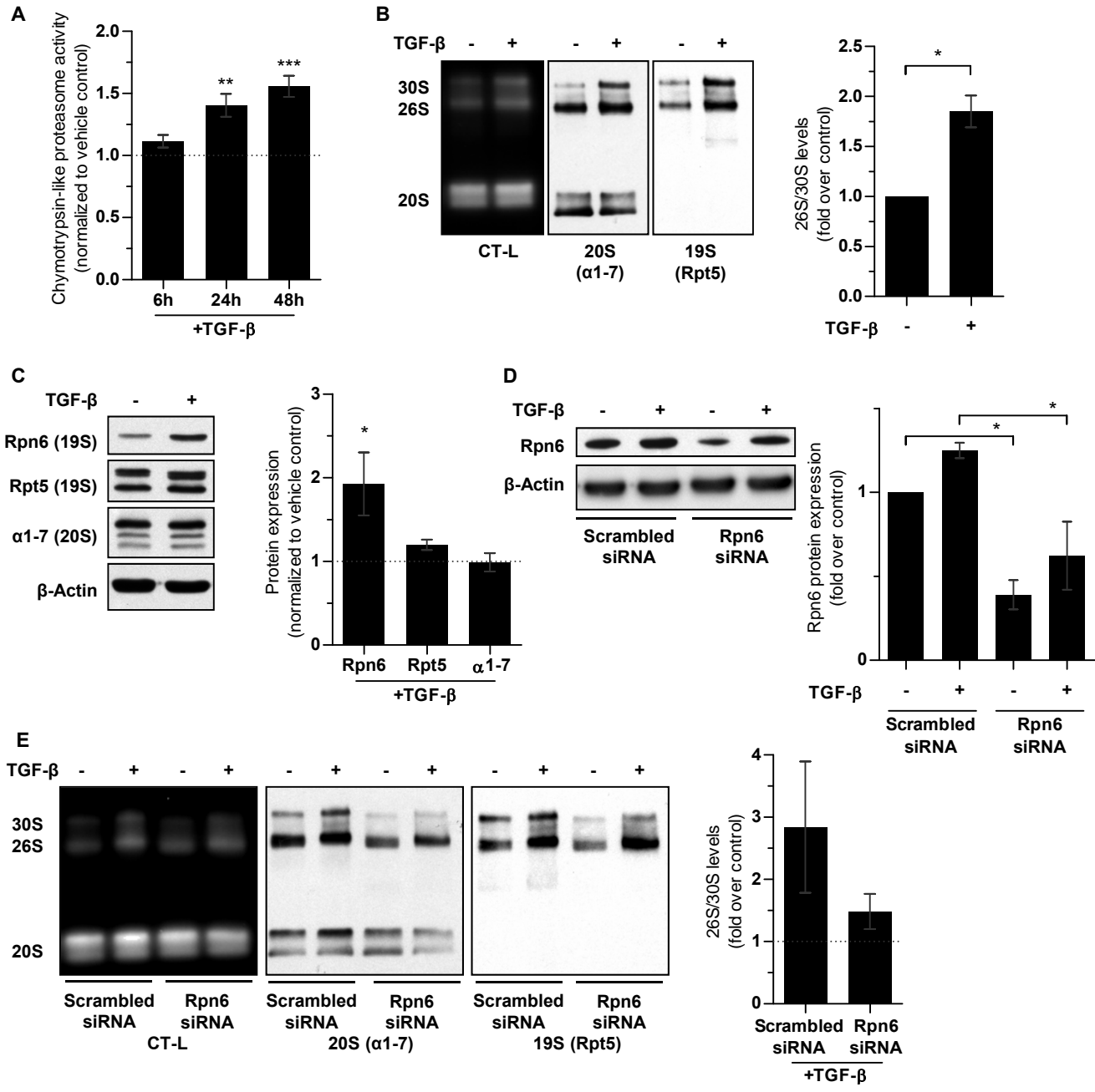
Immunohistochemistry of paraffin-embedded donor and IPF lung tissues stained for Rpn6, KRT5 (basal cell marker), or  $\alpha$ SMA (marker for smooth muscle cells and myofibroblasts). (Rpn6,  $\alpha$ SMA and KRT5: red; Nuclei: blue). Pictures show representative stainings for 10 IPF and 6 donor lungs.

**Fig. 6.** Levels of K48-polyubiquitinated proteins are increased and correlate with Rpn6 upregulation in myofibroblasts and hyperplastic basal cells in human IPF lungs.

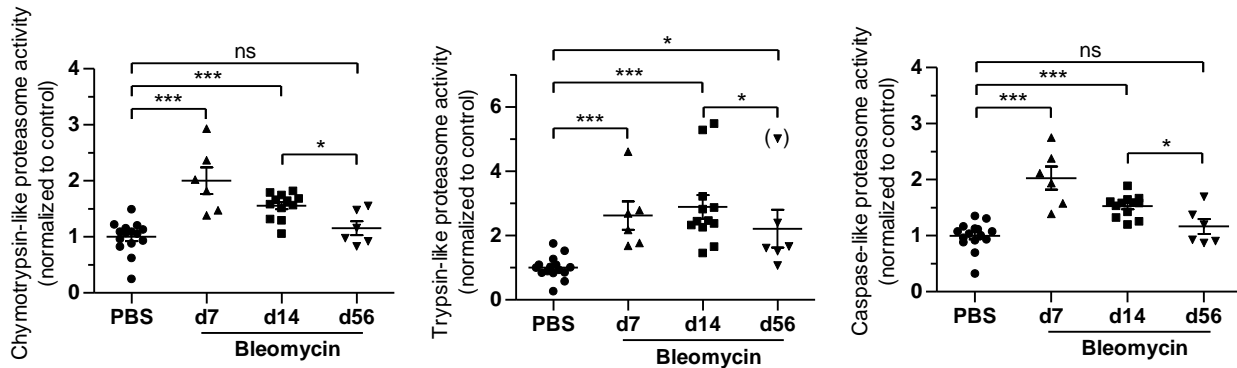
Immunohistochemistry of donor and IPF lungs stained for Rpn6 and K48-polyubiquitinated proteins (Ubi-K48). (Rpn6 and Ubi-K48: red; Nuclei: blue).

**Fig. 7.** Silencing of Rpn6 counteracts TGF- $\beta$  induced myofibroblast differentiation in primary human lung fibroblasts (phLF). **(A)** Native gel analysis of CT-L proteasome activity and immunoblotting for Rpt5 and  $\alpha$ 1-7 ( $n = 3$ ). **(B)** RNA expression of fibrotic markers, i.e. collagen I (Coll-I) and fibronectin (Fn), in phLF treated for 48h with TGF- $\beta$  starting 24h after Rpn6 knockdown as determined by qRT-PCR analysis (Mean  $\pm$  SEM.  $n = 4$ . 1way ANOVA, Bonferroni-Multiple Comparison Test). **(C)** Western blot analysis and densitometric analysis of RIPA lysates for fibronectin (Fn), collagen I (Coll-I), and Rpn6 in phLF after Rpn6 knockdown and TGF- $\beta$  treatment using  $\beta$ -actin protein expression for normalization (Mean  $\pm$  SEM.  $n = 4$ . Two-tailed Mann Whitney Test).

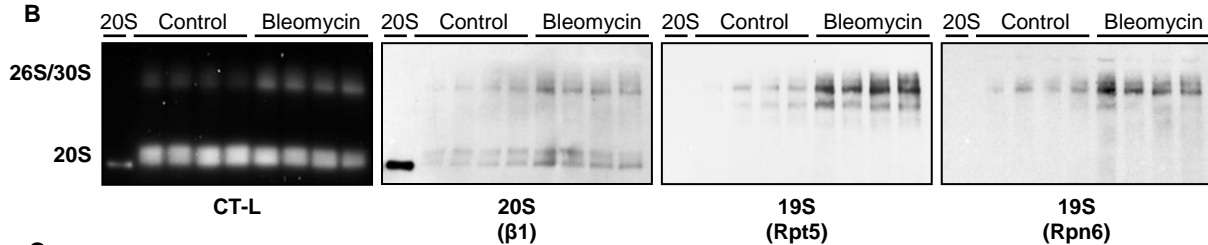
**Fig. 8.** Silencing of Rpn6 inhibits ubiquitin-mediated protein degradation in primary human lung fibroblasts (phLF). Western blot analysis of Rnp6, K48-linked polyubiquitin (Ubi-K48), collagen-1 (Coll-1) and cyclin D1, and densitometric analysis of  $\beta$ -actin normalized expression levels using 6 different lines of phLF knockdown of Rpn6 for 48h (Mean  $\pm$  SEM.  $n = 6$ . Two-tailed paired t-test).



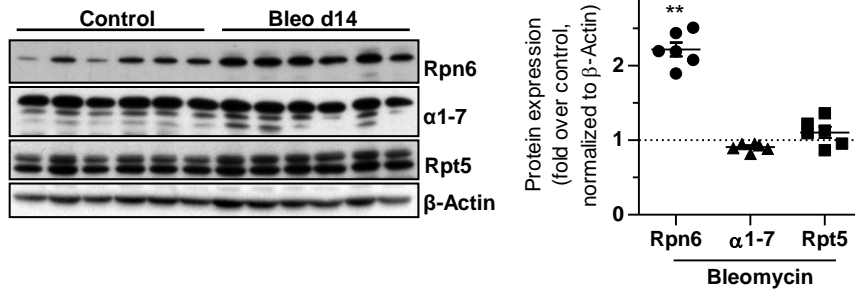
A

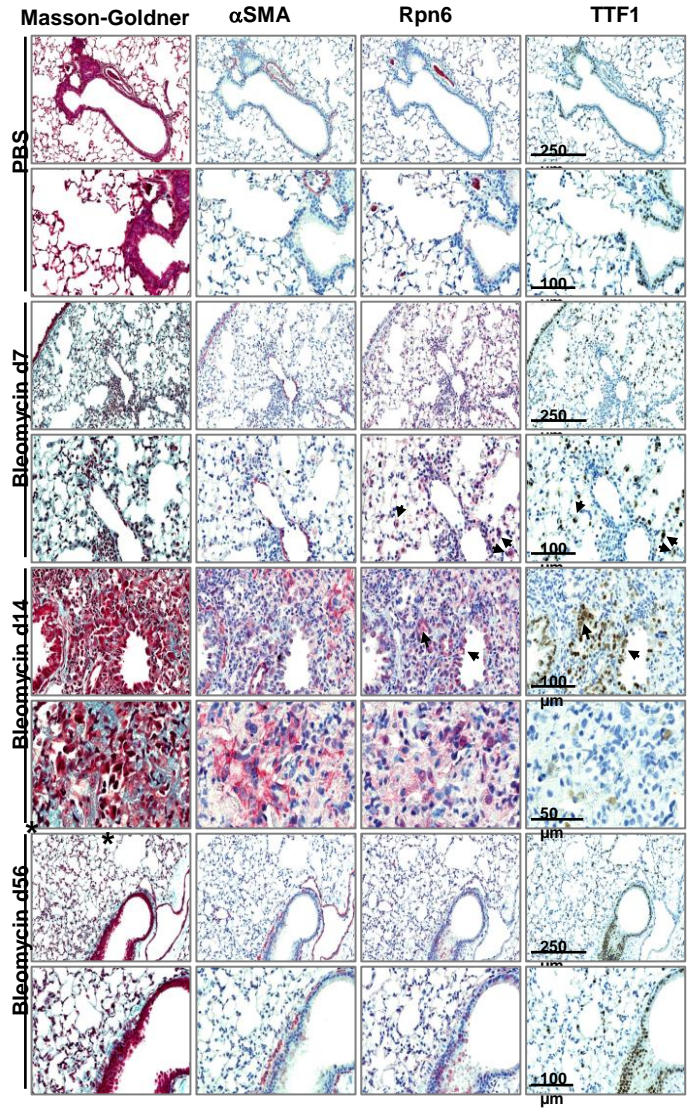


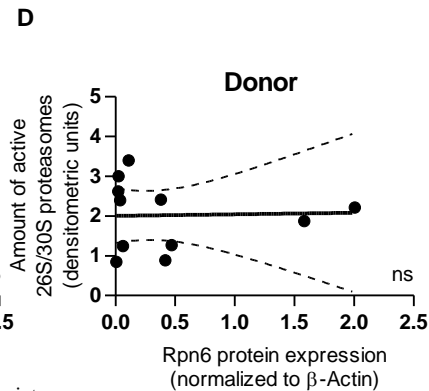
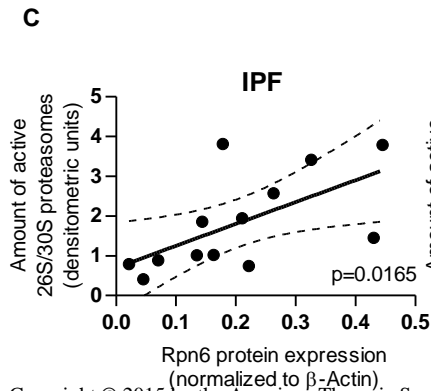
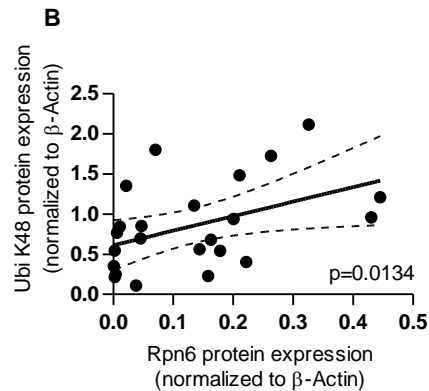
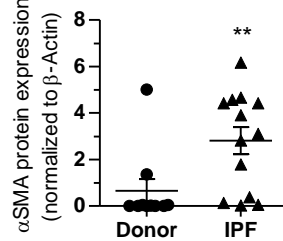
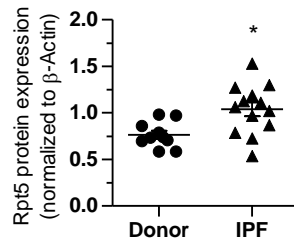
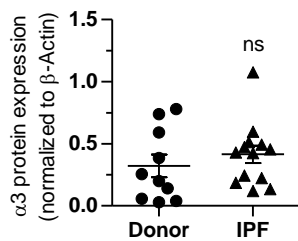
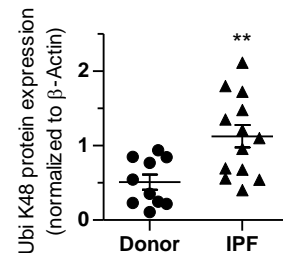
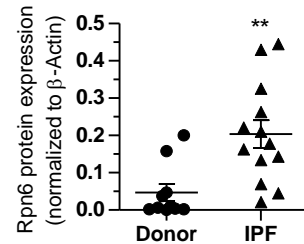
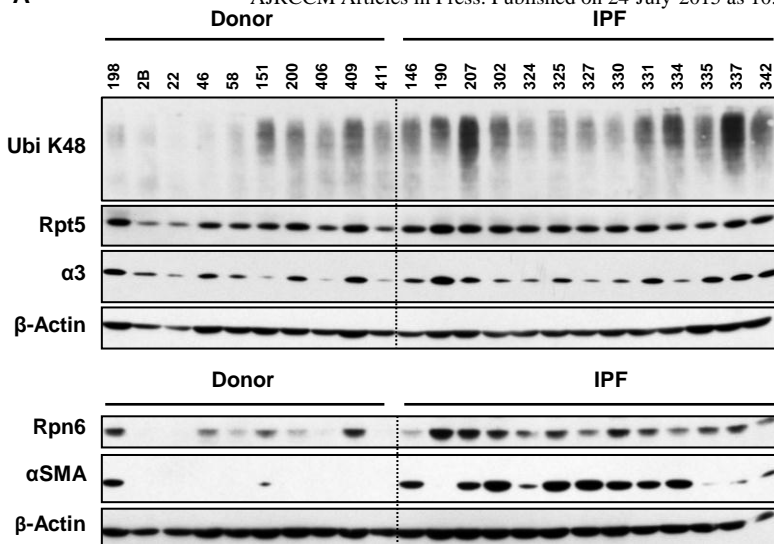
B

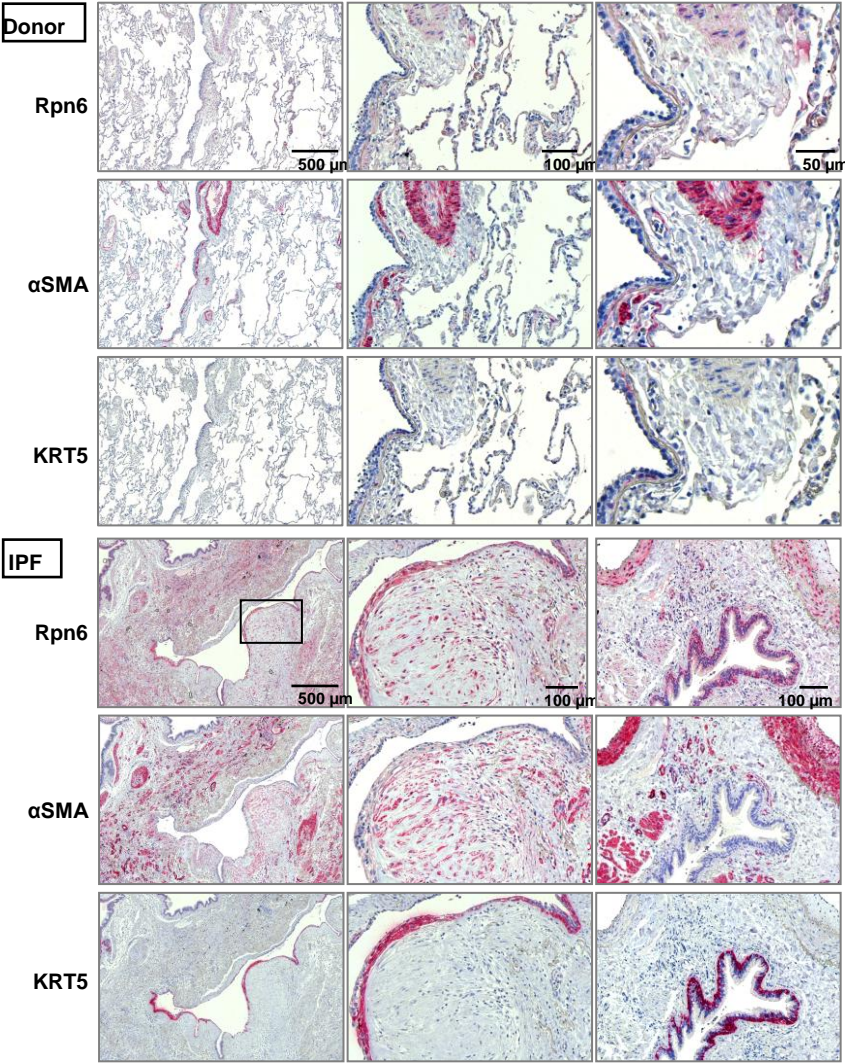


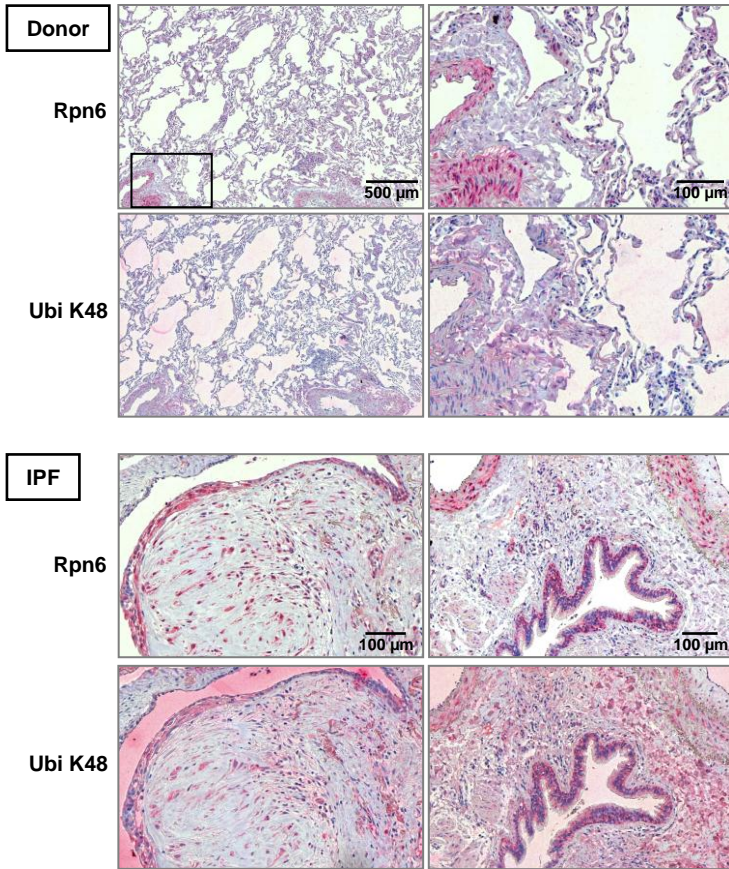
C



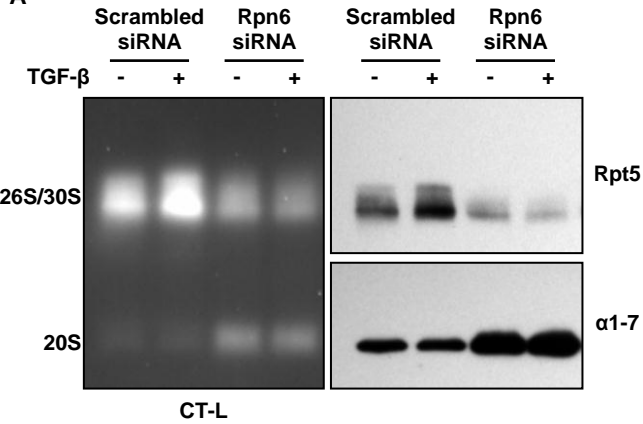




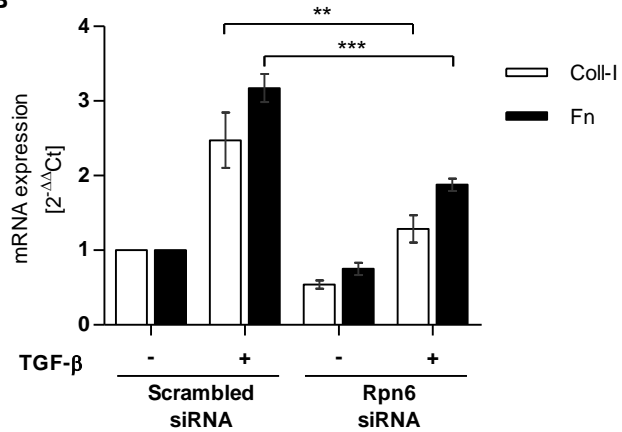




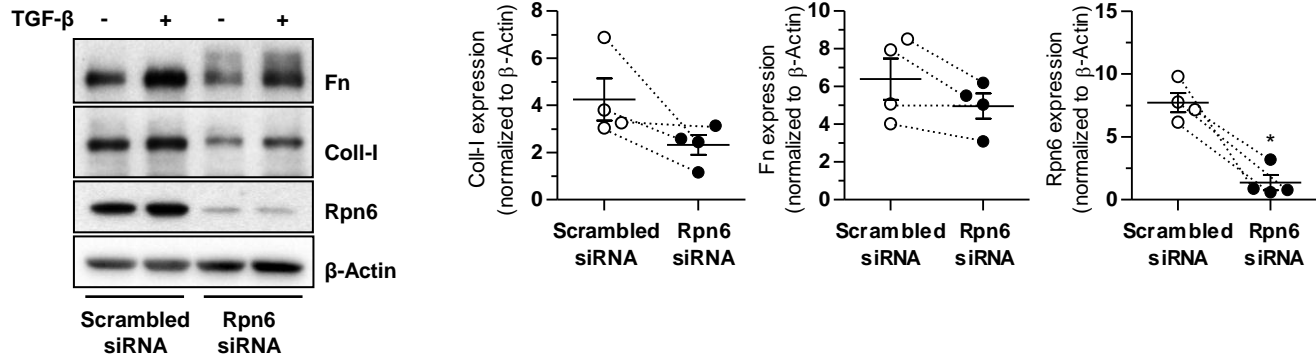
**A**

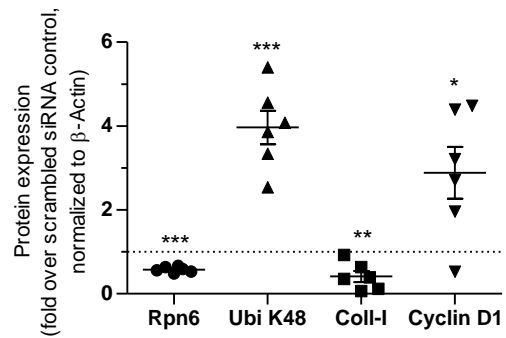
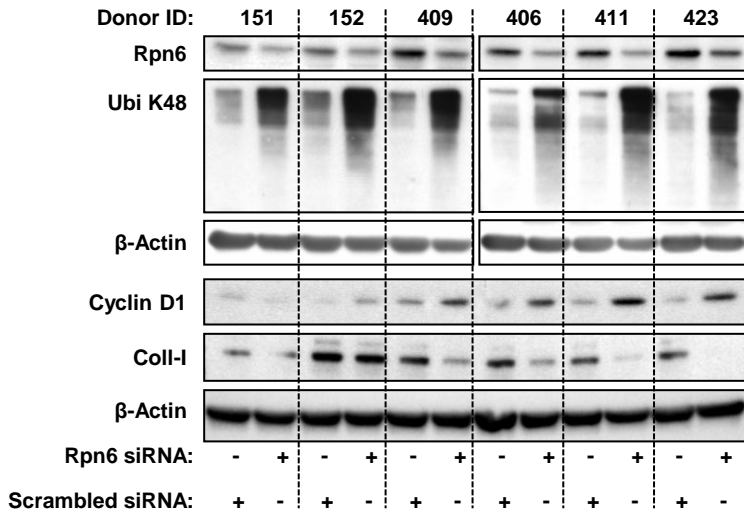


**B**



**C**





## Supplementary Information: Regulation of 26S proteasome activity in pulmonary fibrosis

**Authors:** Nora Semren<sup>1</sup>, Vanessa Welk<sup>1#</sup>, Martina Korfei<sup>2#</sup>, Ilona E. Keller<sup>1</sup>, Isis E. Fernandez<sup>1</sup>, Heiko Adler<sup>3</sup>, Andreas Günther<sup>2,4</sup>, Oliver Eickelberg<sup>1</sup>, Silke Meiners<sup>1\*</sup>

### **Affiliations:**

<sup>1</sup>Comprehensive Pneumology Center (CPC), University Hospital, Ludwig-Maximilians University, Helmholtz Zentrum München, Munich, Member of the German Center for Lung Research (DZL), Germany.

<sup>2</sup>Department of Internal Medicine, Universities of Giessen and Marburg Lung Center (UGMLC), Justus-Liebig-University Giessen, Member of the German Center for Lung Research (DZL), Germany.

<sup>3</sup>Research Unit Gene Vectors, Helmholtz Zentrum München - German Research Center for Environmental Health (GmbH), Munich, Germany

<sup>4</sup>Agaplesion Lung Clinic Waldhof Elgershausen, Greifenstein, Germany, European IPF Network and European IPF Registry.

# both authors contributed equally

\*Corresponding author: Silke Meiners, Max-Lebsche Platz 31, 81377 Munich, Germany, Phone: 00498931874673, silke.meiners@helmholtz-muenchen.de

**One Sentence Summary:** 26S proteasome activity is activated upon myofibroblast differentiation and in pulmonary fibrosis.

## Supplementary Materials and Methods

### *Cell culture and gene silencing*

The CCL206 mouse lung fibroblast cell line was obtained from ATCC and cultured under standard conditions in DMEM-F12 medium (Gibco) supplemented with 10% FBS (PAN Biotech) and 100 U/ml penicillin/streptomycin (Gibco). pHLF at passages 2 and 4 were cultured under standard conditions in MCDB 131 Medium (PAN Biotech) supplemented with 10% FBS (PAN Biotech), 100 U/ml penicillin/streptomycin (Gibco), 2 mM glutamine (Gibco), 2 ng/ml  $\beta$ -FGF (Gibco), 0.5 ng/ml EGF (Sigma-Aldrich) and 5  $\mu$ g/ml Insulin (Gibco). Knockdown experiments of murine Rpn6 in CCL206 mouse lung fibroblasts and of human Rpn6 in pHLF were performed by reverse transfection of small interfering RNA (Silencer Select s87417 or s11413, Ambion) or scrambled siRNA (Silencer Select Control#2, Ambion) using Lipofectamine RNAiMAX (Life Technologies) according to the manufacturer's protocol. Confirmatory experiments in pHLF were performed with a pool of three siRNAs (Silencer Select s11413, s11414, s11415, Ambion) for Rpn6 knockdown and a pool of two scrambled control siRNAs (Silencer Select Control#1 and #2, Ambion).

### *Native gel analysis*

Native gel electrophoresis was performed using the XCell SureLock® Mini-Cell system (Life Technologies). Proteins (30  $\mu$ g of hypoosmotic lysates) were loaded on gradient (3-8% acrylamide) tris-acetate gels (NuPAGE Novex 3-8%, Life Technologies) and run for 4h at 150 V and 4°C. Native gels were incubated for 30 min at 37°C in assay buffer (50 mM Tris, pH 7.5, 10 mM MgCl<sub>2</sub>, 1 mM ATP, 1 mM DTT) containing 50  $\mu$ M Suc-LVVY-AMC (Bachem), a fluorogenic, synthetic peptide substrate of the chymotrypsin-like (CT-L) activity of the proteasome. Gels were imaged at excitation wavelength of 380 nm and emission wavelength of

460 nm in the ChemiDoc XRS+ system (Bio-Rad). Subsequently, gels were blotted onto polyvinylidene difluoride membranes and proteins were detected using standard antigen detection procedures with the ECL Plus Detection Reagent (GE Healthcare) followed by exposure of Kodak X-Omal LS films (Sigma-Aldrich) and development of films in a Curix 60 developer (Agfa) or with the ChemiDoc XRS+ (Bio-Rad).

#### *ABP Proteasome labeling*

In gel proteasome activity was monitored by using the pan-reactive proteasome ABP MV151 (1). TSDG buffer lysates (Tris/HCl 50 mM pH 7.0, NaCl 10 mM, MgCl<sub>2</sub> 1.1 mM, EDTA 0.1 mM, NaN<sub>3</sub> 1 mM, DTT 1 mM, ATP 2 mM, Glycerol 10% (v/v), cOmplete protease inhibitor (Roche) of whole human lung tissue were diluted to a total protein concentration of 0.5 µg/µl with reaction buffer (50 mM HEPES pH 7.4, 100 mM KCl, 10 mM MgCl<sub>2</sub>). 30 µl of sample was incubated with 0.5 µM MV151 for 1h at 37°C and subsequently quenched by the addition of 1x sample buffer. Native gel separation was performed as described above and proteasome activity was visualized using a fluorescent scanner (Typhoon TRIO+; Amersham Biosciences). Images were taken at 450 PTM and 50 µm pixel resolution with fluorescence Cy3/TAMRA for ABPMV151.

#### *Induction and assessment of pulmonary fibrosis*

a) Bleomycin: Pulmonary fibrosis was initiated by a single intratracheal instillation of 50 µl of bleomycin (3U/kg, Sigma Aldrich, Taufkirchen, Germany), that had been dissolved in sterile saline, and locally applied using the MicroSprayer Aerosolizer, Model IA-1C (Penn-Century, Wyndmoor, PA). Control mice were instilled with 50 µl of sterile PBS. Fibrosis was assessed by lung function measurement via Flexivent, broncho-alveolar lavage cell counts, and histology evaluation.

b) MHV-68 infection: Wildtype C57BL/6 mice (Charles River Laboratories, Sulzfeld, Germany) and IFN $\gamma$ R<sup>-/-</sup> mice on a C57BL/6 background (originally purchased from Jackson Laboratories, Bar Harbor, Maine, and bred in the animal facility of the Helmholtz Zentrum München) were anesthetized using ketamine/xylazine and infected intranasally with  $1 \times 10^5$  plaque forming units (PFU) of murine gammaherpesvirus-68 (MHV-68) as described elsewhere (2). Animals were sacrificed at days 45 and 63 after infection. Mice were housed in individually ventilated cages during the MHV-68 infection period. All animal experiments were in compliance with the German Animal Welfare Act, and the protocol was approved by the local Animal Care and Use Committee (District Government of Upper Bavaria; permit number 124/08).

#### *Immunohistochemistry (IHC)*

Human and mouse lungs were fixed in 4% (w/v) paraformaldehyde and processed for paraffin embedding. Sections (3  $\mu$ m) were cut, mounted on glass slides (Super Frost Plus), and cooked in 10 mM sodium citrate-buffer (pH 6.0). Proteins were immunostained using the ZytoChem-Plus AP Kit (Fast Red) or ZytoChem-Plus HRP Kit (DAB-staining, brown dye), Broad Spectrum (Zytomed Systems) according to the protocol as previously described (3). The following primary antibodies were used against Cytokeratin-5 [KRT5] (Abcam),  $\alpha$ SMA (Abcam), Rpn6 (Novus Biologicals), Lys48-Ubiquitin [K48] (Millipore) and TTF1 (Abcam). Counterstaining was performed using Mayer's hemalaun solution (WALDECK Division CHROMA). To assess fibrotic remodelling in bleomycin challenged animals, standard Masson-Goldner staining was performed using Weigert's hematoxylin (PolyScience), Ponceau de Xylidene (Waldeck), Orange G (Waldeck) and Light Green (Waldeck). Control sections were treated with PBS containing 2% BSA or with rabbit primary antibody isotype control (Acris Antibodies). Sections were scanned with a Mirax Desk slide scanning device (Zeiss). IHC was performed for 10 IPF-

and 6 control lung tissue samples. Lungs of 3 PBS treated control animals and 14 bleomycin challenged animals (4 animals after 7 days, 6 animals after 14 days and 4 animals after 56 days of bleomycin instillation) were analysed by IHC.

#### *BrdU cell proliferation assay*

BrdU cell proliferation assay (Roche) was performed according to the manufacturer's protocol. Briefly, reverse transfection with siRNA was performed and cells were plated at a density of 2000 cells/well in 100  $\mu$ l transfection medium in a 96 well plate. The next day, transfection medium was replaced by culture medium containing 1% FBS and 5 ng/ml TGF- $\beta$ . 48h later cells were labeled for 2-4h using 10  $\mu$ M BrdU, cells were dried and stored at 4°C overnight. The next day, cells were fixed and DNA was denatured by adding FixDenat and incubated with anti-BrdU-POD antibody for 90 minutes at room temperature. Cells were washed and substrate solution was added. The reaction was stopped by adding H<sub>2</sub>SO<sub>4</sub> to a final concentration of 0.2 M. Absorbance measurement was performed within 5 minutes at 450 nm using a Tristar LB 941 plate reader (Berthold Technologies).

#### *RNA preparation*

Frozen mouse or human lung tissue samples were homogenized using a Mikro-Dismembrator S (Sartorius). Tissue powder was suspended in Solution 1 of the Rota-Quick-Kit (A979.1, Carl Roth) and incubated on ice to allow cell lysis. RNA extraction was performed by phase separation using Solution 2 of the Rota-Quick-Kit according to the manufacturer's protocol. In a next step RNA was purified using the Peqlab-Gold Total RNA-Kit (12-6834-01, Peqlab) according to the manufacturer's protocol starting with loading of the prepared RNA extract on the RNA-binding column. Reverse transcription and quantitative PCR reaction were performed as described in the material and methods part.

**Fig. E1.** TGF- $\beta$  mediated increase in proteasome activity can be counteracted by inhibition of the proteasome. Chymotrypsin-like (CT-L) activity in cell lysates of CCL206 fibroblasts treated with TGF- $\beta$  for 48h and additional incubation with 10 nM bortezomib for 1.5h (Mean  $\pm$  SEM.  $n = 4$ . One-way ANOVA, Bonferroni's Multiple Comparison Test).

**Fig. E2.** TGF- $\beta$  reproducibly increases 26S/30S proteasome formation in CCL206 fibroblasts. Native gel analysis with subsequent CT-L activity assay and immunblotting for  $\alpha$ 1-7 20S subunits from two other independent additional experiments complementary to Figure 1B.

**Fig. E3.** Morphological changes in CCL206 murine lung fibroblasts after Rpn6 silencing and TGF- $\beta$  treatment as observed by phase-contrast light microscopy. CCL206 fibroblasts were treated for 48h with TGF- $\beta$  (5 ng/ml) starting 24h after Rpn6 knockdown.

**Fig. E4.** Rpn6 silencing reproducibly inhibits TGF- $\beta$ -induced activation of 26S/30S proteasome formation in CCL206 fibroblasts. Native gel analysis with CT-L activity assay and immunoblotting for Rpt5 and  $\alpha$ 1-7 from independent additional silencing experiments complementary to Figure 1E.

**Fig. E5.** 20S levels are not affected by Rpn6 silencing in TGF- $\beta$  treated CCL206 fibroblasts. 20S levels were analyzed by densitometry of the 20S  $\alpha$ 1-7 immunoblots of the native gels as shown in Figures 1E and E4 (Mean  $\pm$  SEM.  $n = 4$ . One-way ANOVA, Bonferroni's Multiple Comparison Test)

**Fig. E6.** Lung function analysis (compliance) of bleomycin treated C57BL/6N mice at day 7, 14, and 56 after instillation compared to PBS treated control mice (Mean  $\pm$  SEM.  $n = 6-9$  per group. Two-tailed Mann Whitney Test).

**Fig. E7:** mRNA expression of several proteasomal subunits is not significantly altered in bleomycin-treated C57BL/6N mice. qRT-PCR of whole lung tissue of animals 14 days after bleomycin instillation compared to PBS-treated controls (Mean  $\pm$  SEM.  $n = 6$  per group. Two-tailed Mann Whitney Test).

**Fig. E8.** Rpn6 is overexpressed in lungs of MHV-68 challenged IFN $\gamma$ R<sup>-/-</sup> mice. Western blot analysis of Rpn6,  $\alpha$ 3, and  $\alpha$ SMA in whole lung tissue of MHV-68 challenged wt and IFN $\gamma$ R<sup>-/-</sup> mice lysed in RIPA buffer and corresponding densitometric analyses (Mean  $\pm$  SEM.  $n = 3$ . One-way ANOVA Dunnett's-Multiple Comparison Test).

**Fig. E9.** 26S/30S formation is increased in lungs of MHV-68 challenged IFN $\gamma$ R<sup>-/-</sup> mice. Native gel, CT-L activity overlay assay, and immunoblot analyses for Rpn6 and  $\beta$ 5 of whole lung tissue of MHV-68 challenged wt and IFN $\gamma$ R<sup>-/-</sup> mice lysed in TSDG buffer.

**Fig. E10.** mRNA expression of proteasome subunits is not significantly altered in IPF lungs. qRT-PCR analysis of whole lung tissue of donor and IPF lungs (Mean  $\pm$  SEM.  $n = 8$  donors and  $n = 13$  IPF patients. Two-tailed Mann Whitney Test).

**Fig. E11.** Proteasome activities in IPF lungs are heterogeneous and not altered compared to donor lungs. ABP labelling of proteasomes in whole lung extracts and subsequent native gel analysis (Donor 35 was excluded from analysis as a case of chronic thromboembolic pulmonary hypertonia). Samples were labeled and run in parallel on two gels but imaged at the same time to allow for comparable exposure and densitometric analysis of signals (Mean  $\pm$  SEM.  $n = 10$  donors and  $n = 13$  IPF patients. Two-tailed Mann Whitney Test).

**Fig. E12.** Expression and localization of Rpn6 and  $\alpha$ SMA in lungs of patients with fibrotic NSIP (fNSIP), EAA, or sarcoidosis. Rpn6 expression was virtually absent in fNSIP-lungs, and

not detectable in the interstitial smooth muscle (indicated by  $\alpha$ SMA-staining in a serial section) of thickened alveolar septae (female fNSIP-patient, 51 years old at time of diagnosis). Similarly, interstitial  $\alpha$ -SMA expressing smooth muscle cells in thickened alveolar septae of patients with EAA revealed no notable staining for Rpn6 (female EAA-patient, 50 years old at time of diagnosis). In a sarcoidosis-lung, epitheloid giant granulomas (indicated by asterisks) and some surrounding myofibroblasts (indicated by  $\alpha$ SMA staining) showed weak expression of Rpn6 (male sarcoidosis-patient, 35 years old at time of diagnosis). Results are representative for 3 fNSIP-patients (Mean age  $\pm$  SD,  $53.3 \pm 3.2$  years; 2 females, one male), and for 3 EAA-patients (Mean age  $\pm$  SD,  $51.0 \pm 6.6$  years; 3 females) and one sarcoidosis patient (male sarcoidosis-patient, 35 years old).

**Fig. E13.** Native gel, CT-L activity, and immunoblot analyses of three independent experiments in three different lines of pHLF using a pool of three Rpn6 siRNAs and a pool of two control siRNAs demonstrates the reproducibility of the effects of Rpn6 silencing on TGF- $\beta$  induced 26S/30S proteasome formation as shown in Figure 7A. Densitometric analysis of the amount of 20S and 26S/30S proteasomes calculated from  $\alpha$ 1-7 or Rpt5 immunoblots, respectively. Results were normalized to their scrambled siRNA/non-TGF- $\beta$  control (Mean  $\pm$  SEM.  $n = 3$ . One-way ANOVA Bonferroni-Multiple Comparison Test).

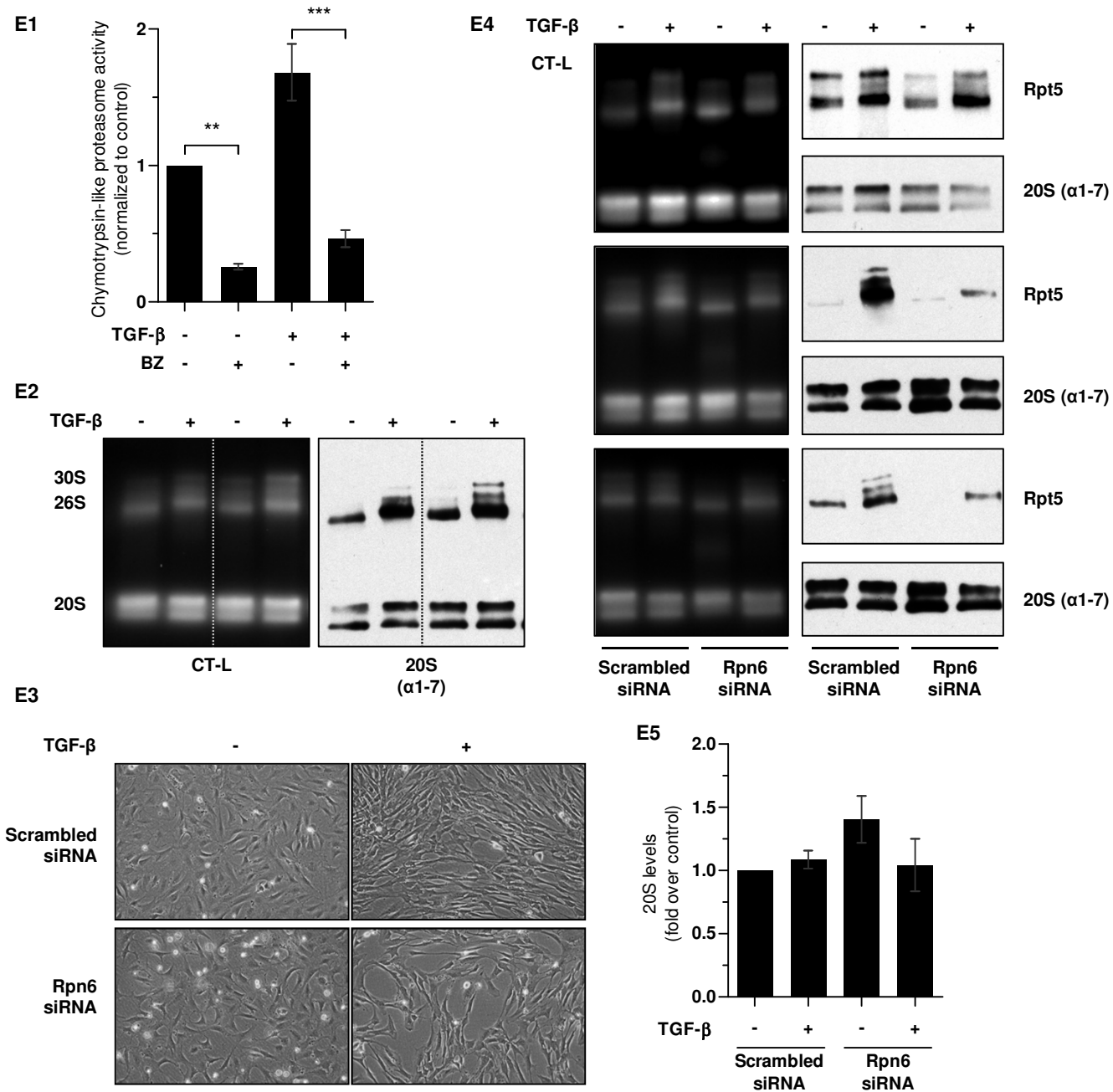
**Fig. E14.** Rpn6 silencing using a pool of three Rpn6 siRNAs and a pool of two control siRNAs confirms the antifibrotic effects in three different TGF- $\beta$  stimulated pHLF lines. mRNA expression of Collagen I (Coll-I) and  $\alpha$ SMA as determined by qRT-PCR analysis (Mean  $\pm$  SEM.  $n = 3$ . One-way ANOVA Bonferroni's-Multiple Comparison Test).

**Fig. E15.** Rpn6 silencing using a pool of three Rpn6 siRNAs and a pool of two control siRNAs confirms the antiproliferative effects in three different TGF- $\beta$  stimulated phLF lines. Protein expression of Rpn6, Cyclin D1, K48-polyubiquitinated proteins, and  $\beta$ -actin was assessed by immunoblotting. Densitometric data were first normalized to the respective  $\beta$ -actin loading control and then to the scrambled siRNA/non-TGF- $\beta$  control (Mean  $\pm$  SEM.  $n = 3$ . One-way ANOVA Bonferroni's-Multiple Comparison Test).

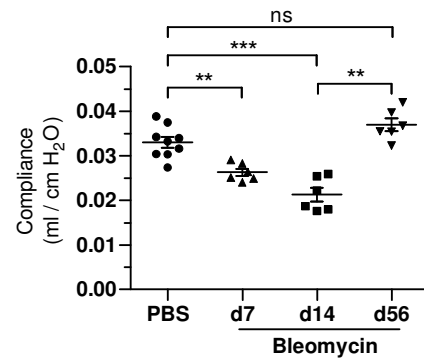
**Fig. E16.** Rpn6 knockdown counteracts TGF- $\beta$  mediated induction in proliferation. BrdU assay of CCL206 fibroblasts treated for 48h with TGF- $\beta$  (5 ng/ml) starting 24h after Rpn6 knockdown (Mean  $\pm$  SEM.  $n = 3$ . One-way ANOVA Bonferroni-Multiple Comparison Test).

### Supplementary References

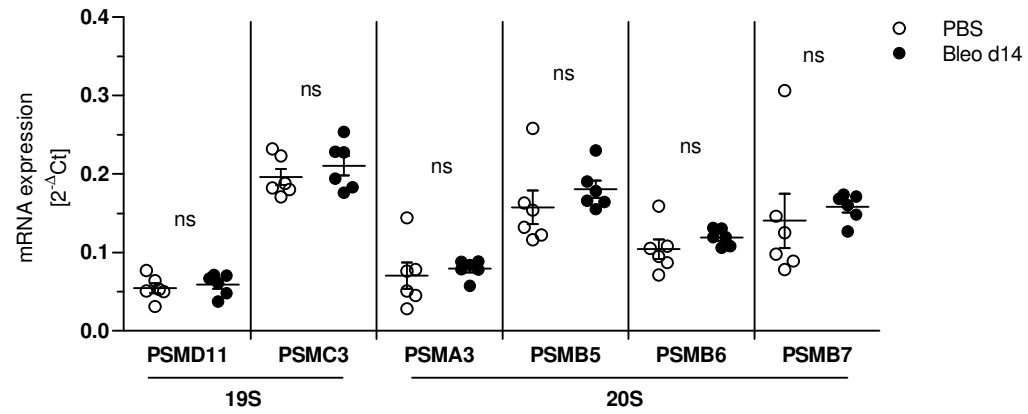
1. Verdoes M, Florea BI, Menendez-Benito V, Maynard CJ, Witte MD, van der Linden WA, van den Nieuwendijk AMCH, Hofmann T, Berkers CR, van Leeuwen FWB, Groothuis TA, Leeuwenburgh MA, Ovaa H, Neefjes JJ, Filippov D V., van der Marel GA, Dantuma NP, Overkleeft HS. A Fluorescent Broad-Spectrum Proteasome Inhibitor for Labeling Proteasomes In Vitro and In Vivo. *Chem Biol* 2006;13:1217–1226.
2. Guggemoos S, Hangel D, Hamm S, Heit A, Bauer S, Adler H. TLR9 contributes to antiviral immunity during gammaherpesvirus infection. *J Immunol* 2008;180:438–443.
3. Korfei M, Schmitt S, Ruppert C, Henneke I, Markart P, Loeh B, Mahavadi P, Wygrecka M, Klepetko W, Fink L, Bonniaud P, Preissner KT, Lochnit G, Schaefer L, Seeger W, Guenther A. Comparative proteomic analysis of lung tissue from patients with idiopathic pulmonary fibrosis (IPF) and lung transplant donor lungs. *J Proteome Res* 2011;10:2185–205.



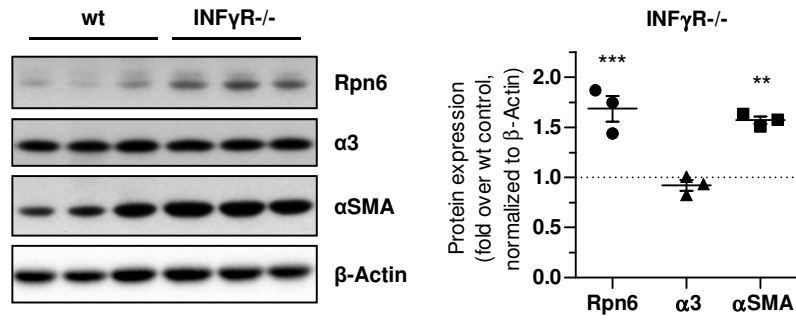
E6



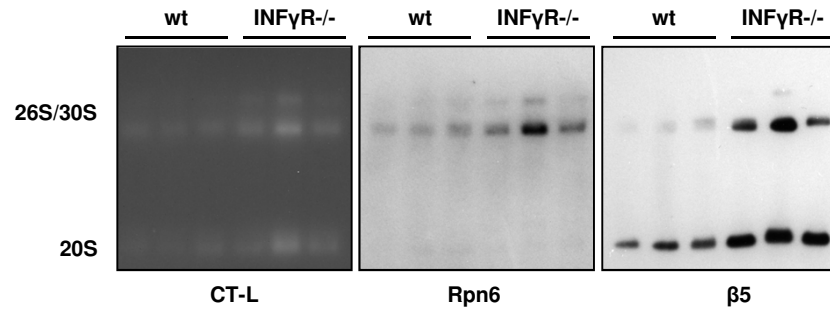
E7

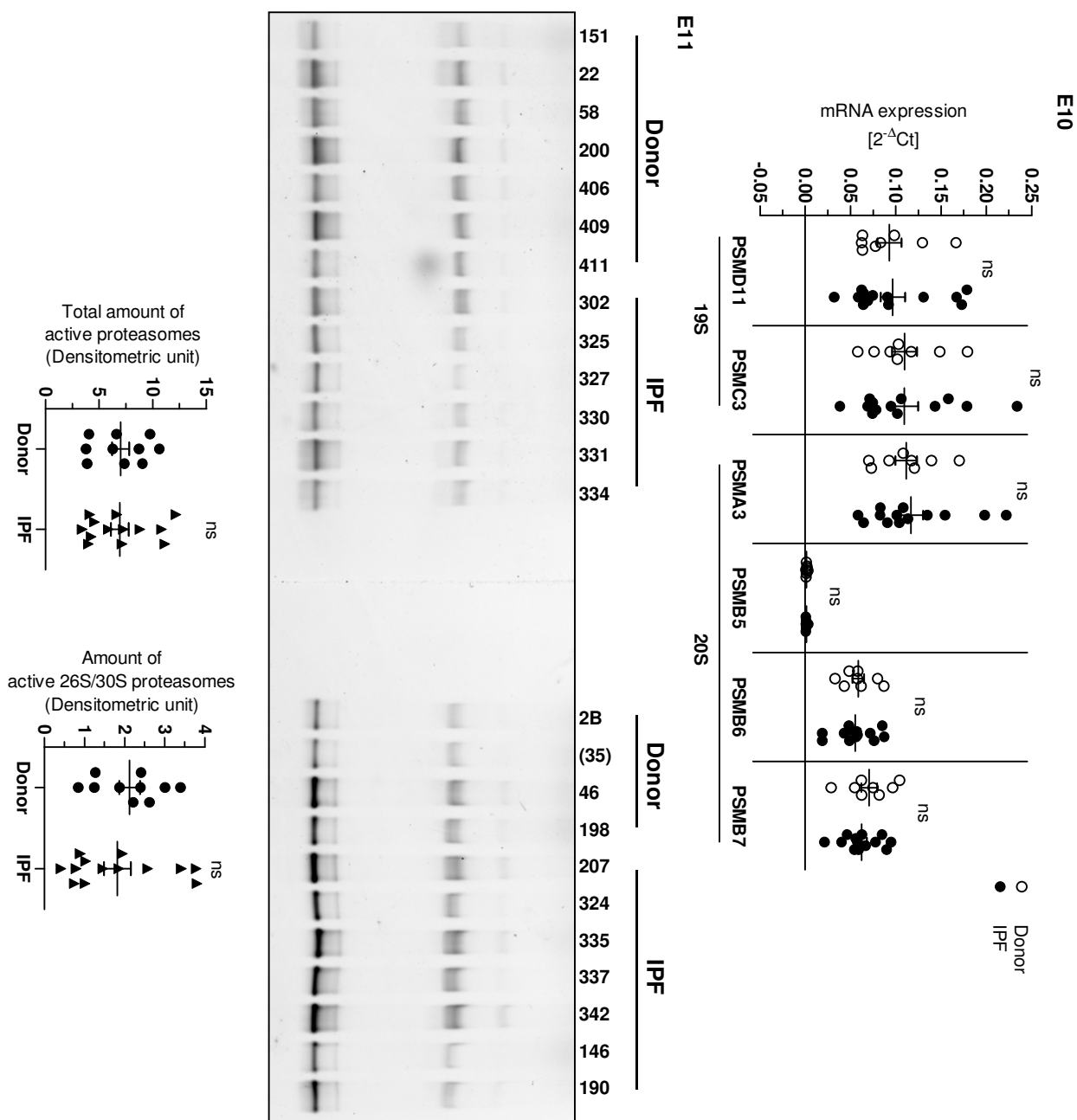


E8



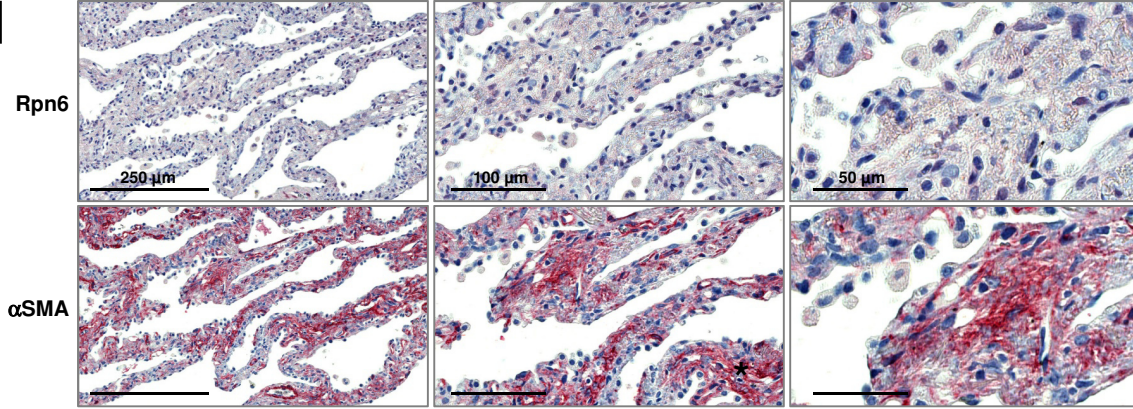
E9



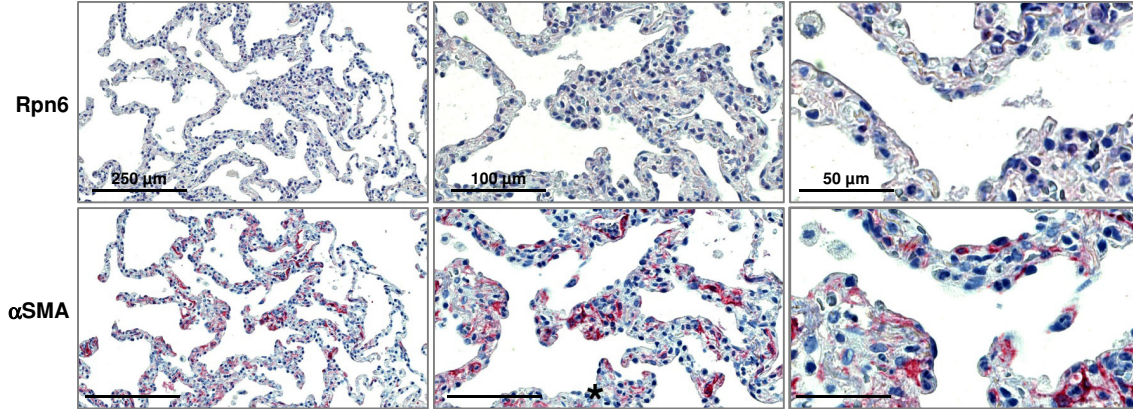


E12

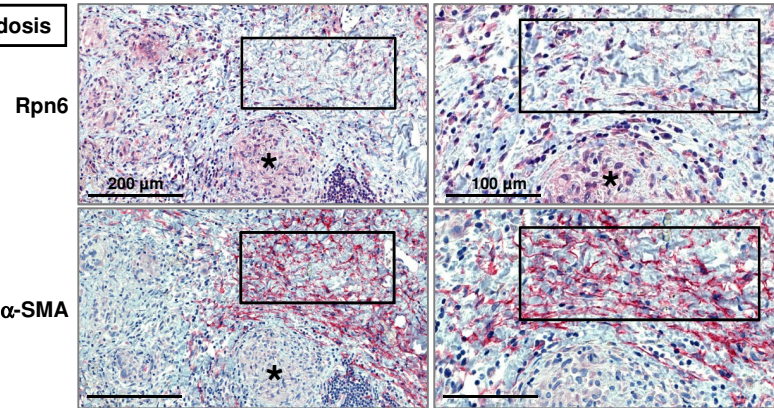
fNSIP



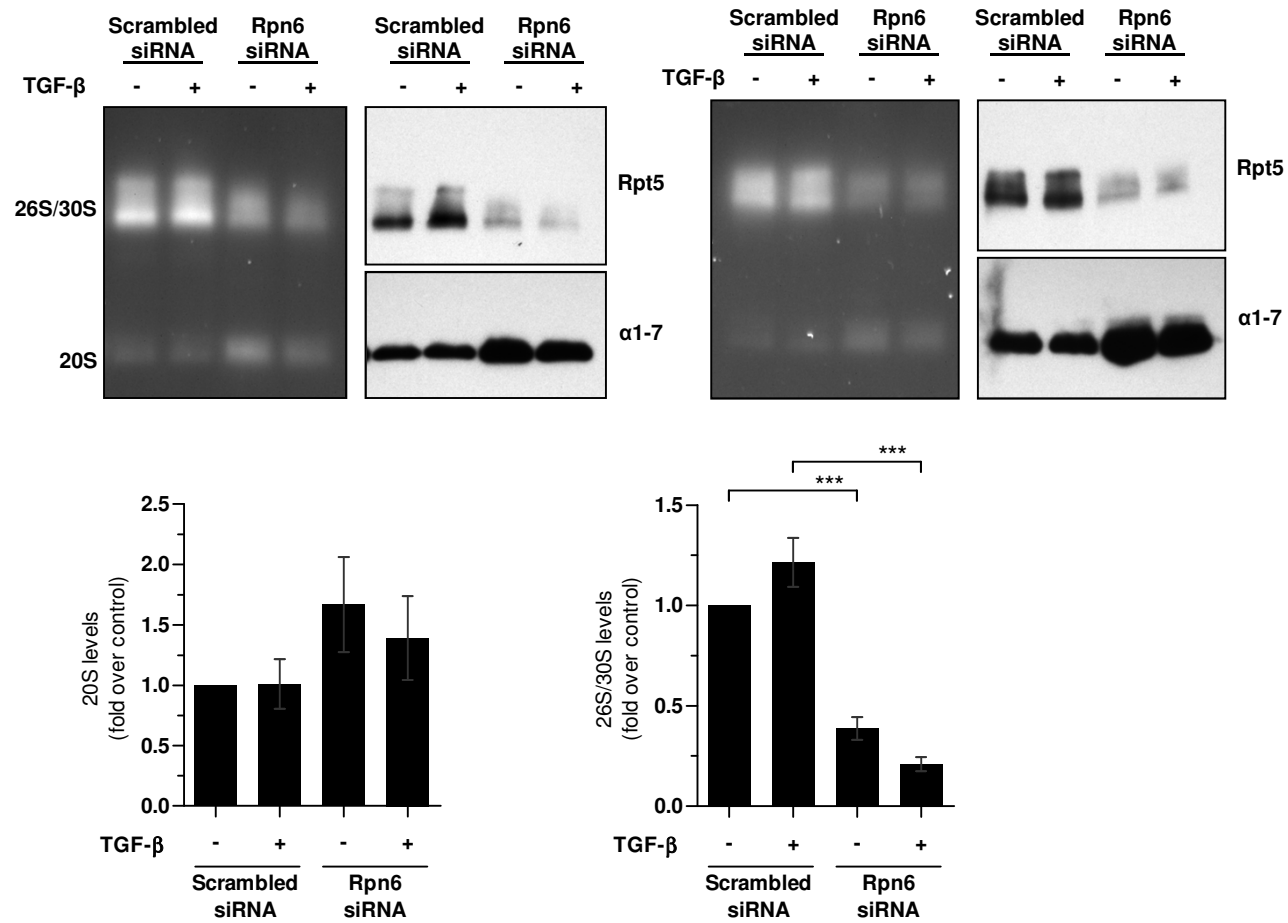
EAA



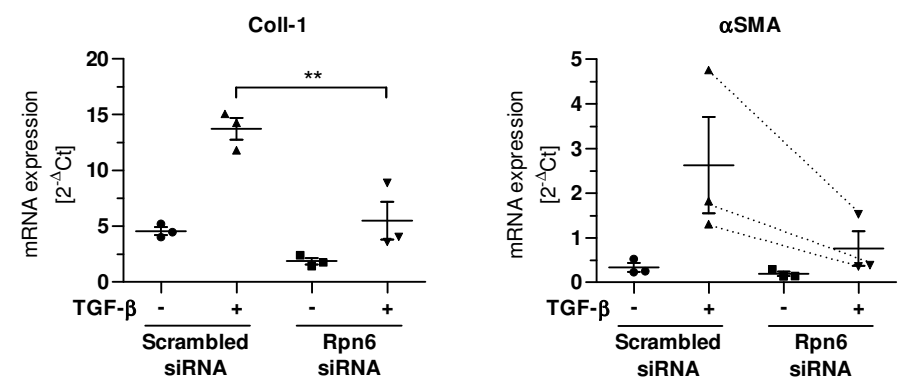
Sarcoidosis



E13



E14



E15

